Impacts of Elastoplasticity and Compliant Zones on the Mechanics of Near-Surface Faulting

Josie Nevitt

USGS Earthquake Science Center, Menlo Park CA

Ben Brooks, Rufus Catchings, Mark Goldman, Dave Lockner, Joanne Chan, Coyn Criley, Sarah Minson, Todd Ericksen, Craig Glennie

Bolinas, CA 1906

G.K. Gilbert

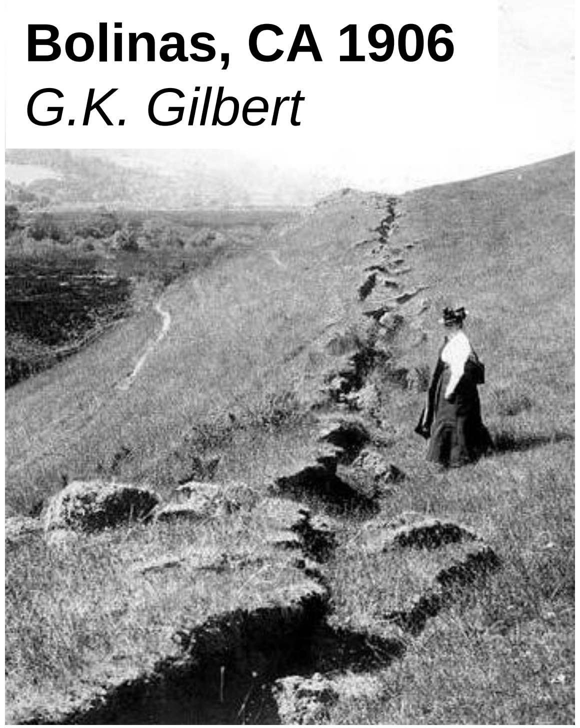

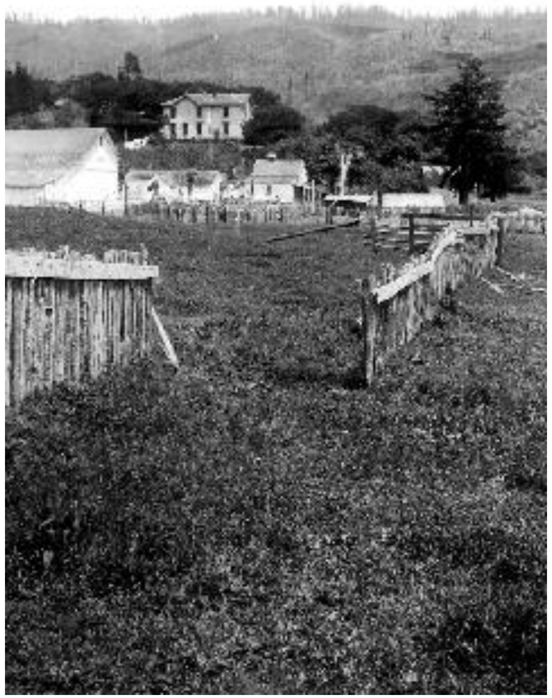

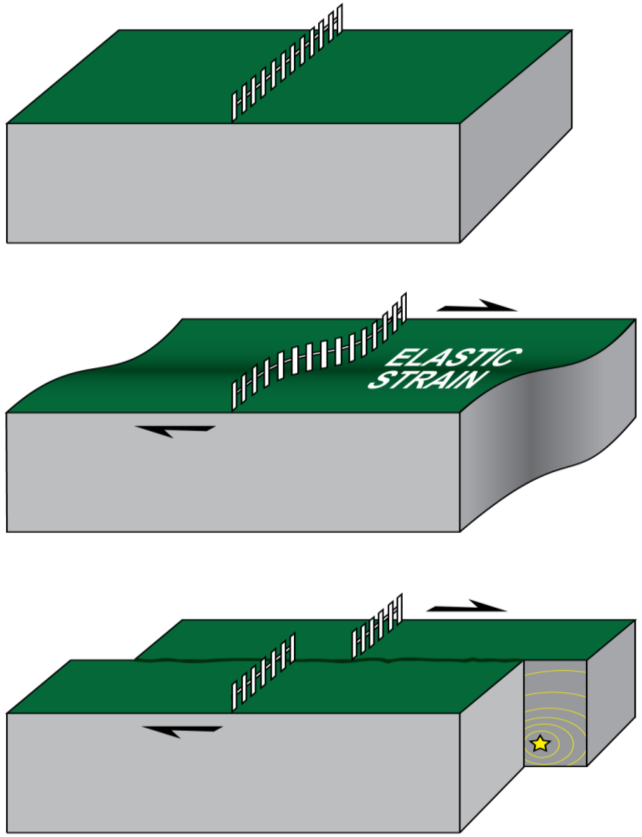

Reid [1910]

Impacts of Elastoplasticity and Compliant Zones on the Mechanics of Near-Surface Faulting

Josie Nevitt

USGS Earthquake Science Center, Menlo Park CA

Ben Brooks, Rufus Catchings, Mark Goldman, Dave Lockner, Joanne Chan, Coyn Criley, Sarah Minson, Todd Ericksen, Craig Glennie

Bolinas, CA 1906

G.K. Gilbert

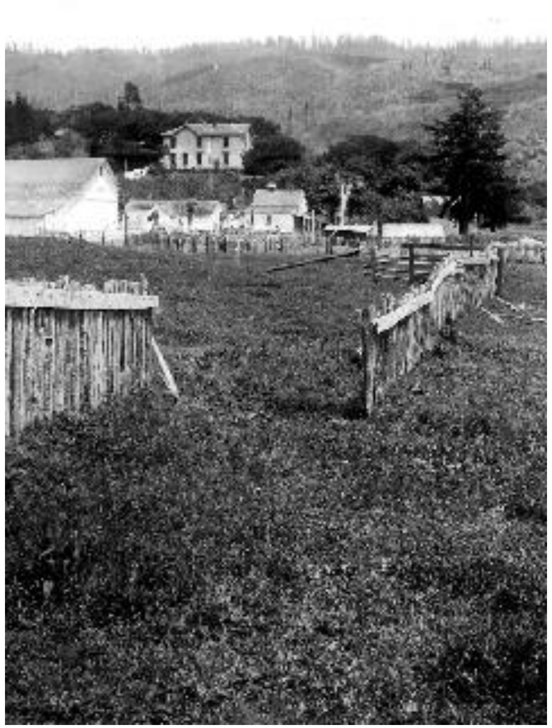

Fault drag [*Lawson et al.*, 1908]

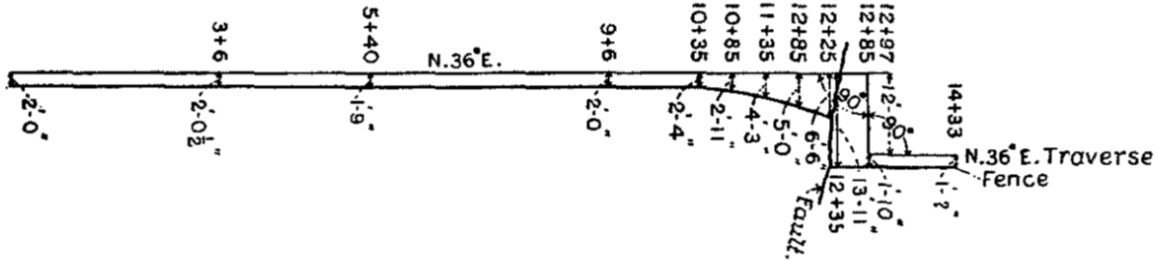

Surface displacement in alluvium [*Reid*, 1910]

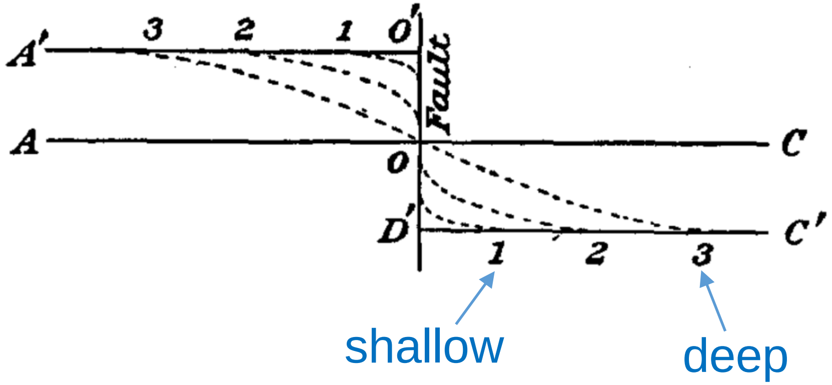

1. What is the magnitude and distribution of shallow fault slip?

Hazard Implication:
Long-term slip rates derived from surface measurements

"Shallow Slip Deficit (SSD)"

Landers (1992)

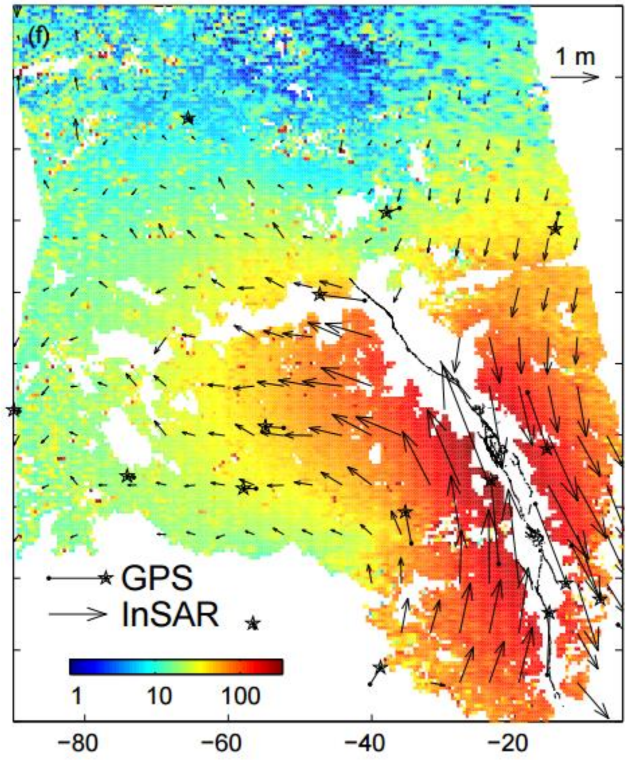

Fialko [2004]

Hector Mine (1999)

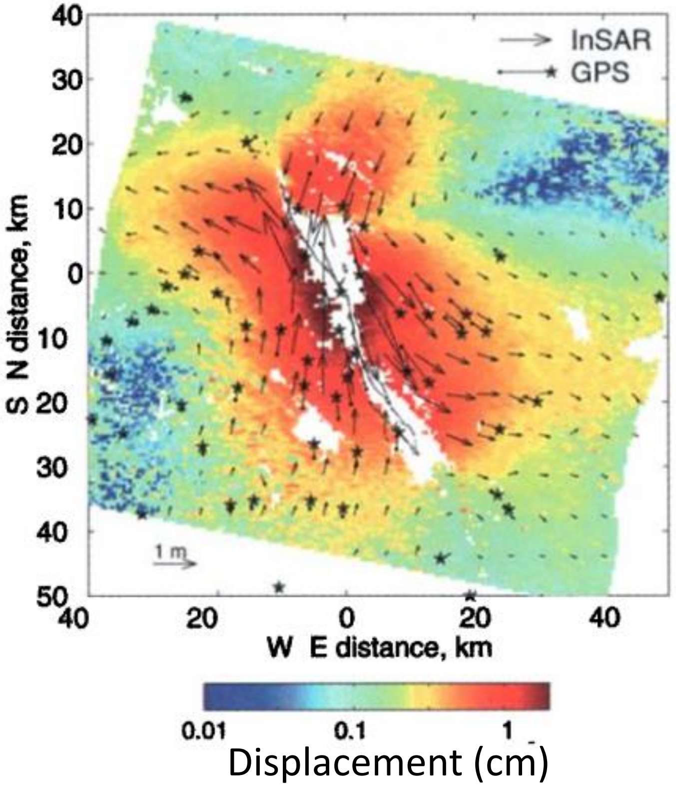

Fialko & Simons [2001]

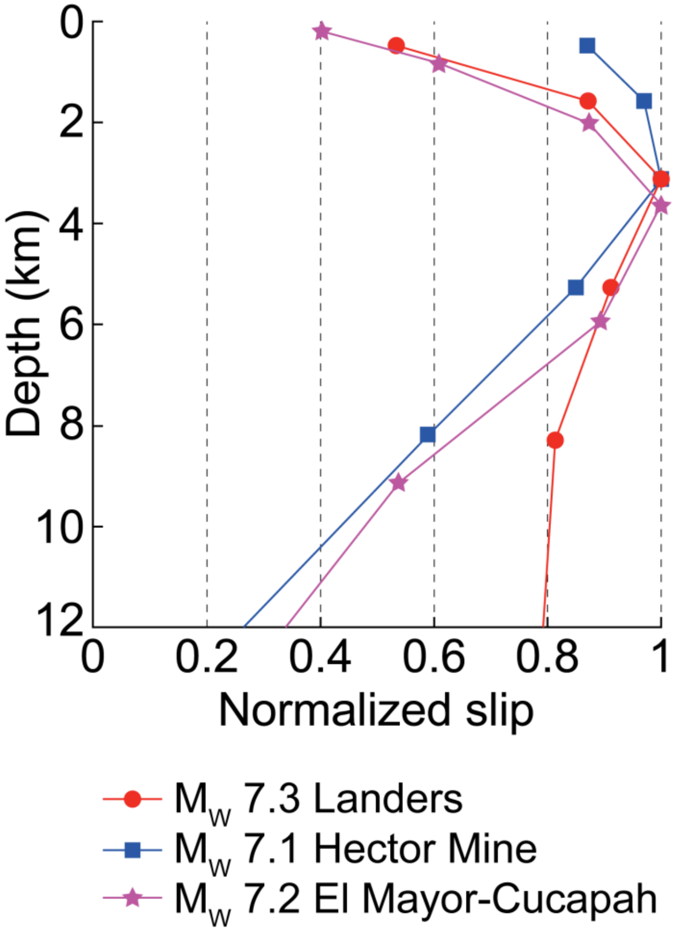

Modified from *Fialko et al.* [2005]

Near-field data critical to resolving shallow slip

SSD = 15-60%

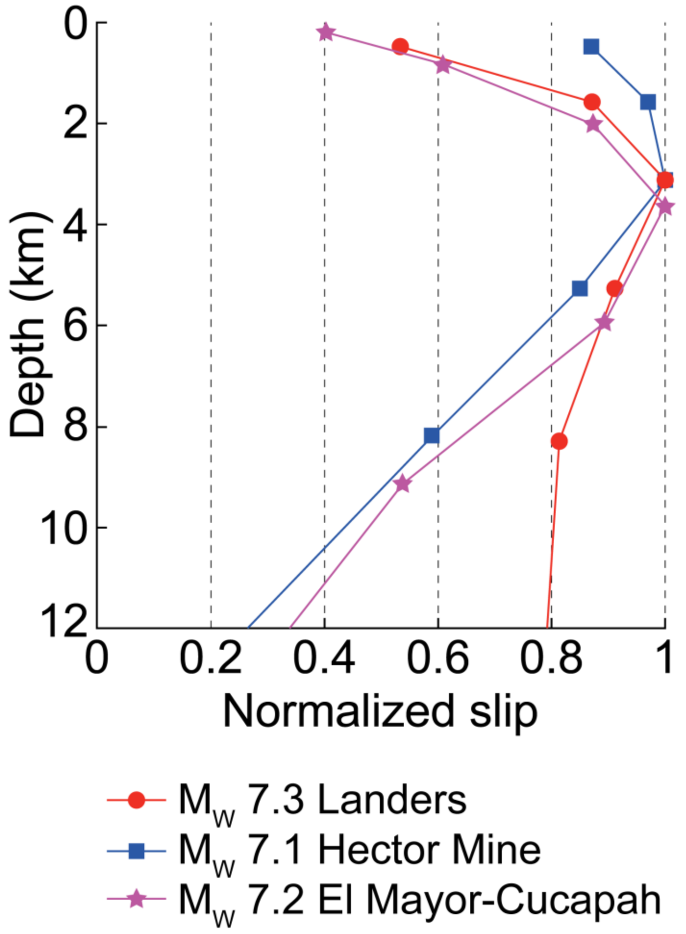

Modified from *Fialko al.* [2005]

Landers

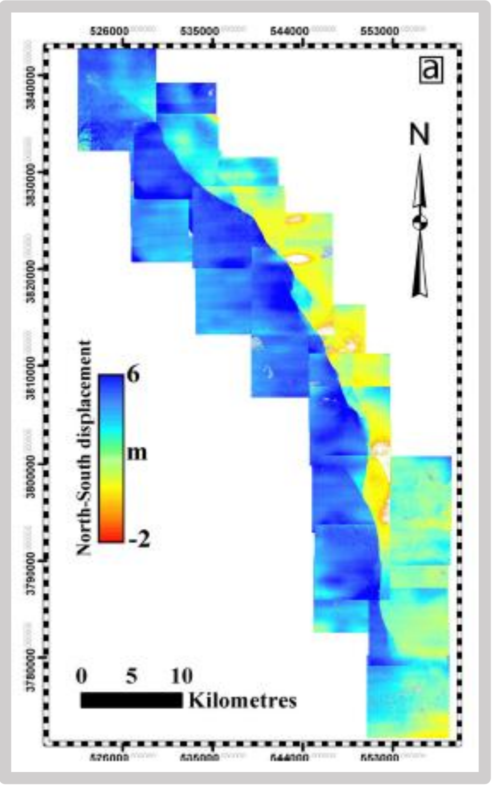

NEAR-FIELD DATA

Milliner et al. [2015]

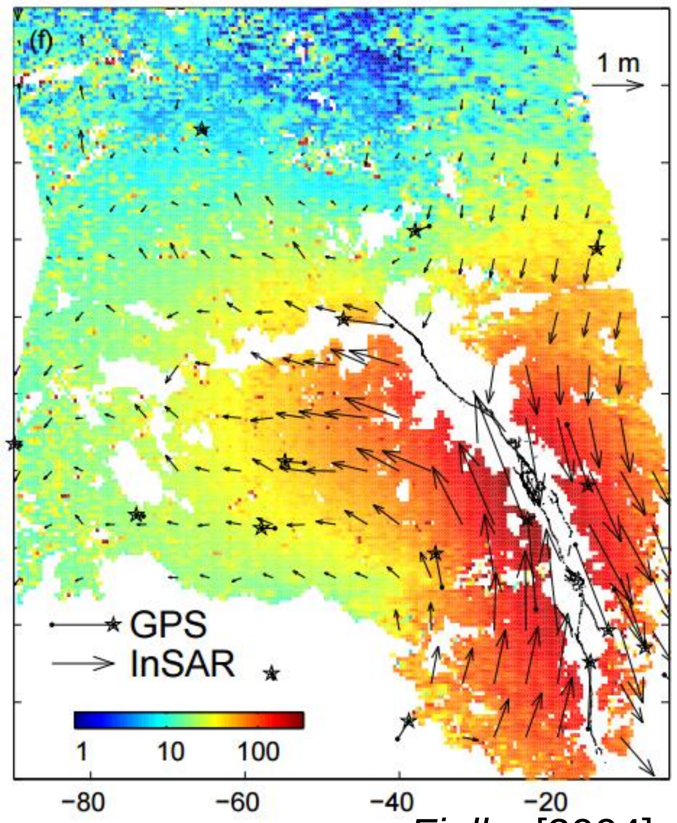

Fialko [2004]

Near-field data critical to resolving shallow slip

SSD = 15-60%

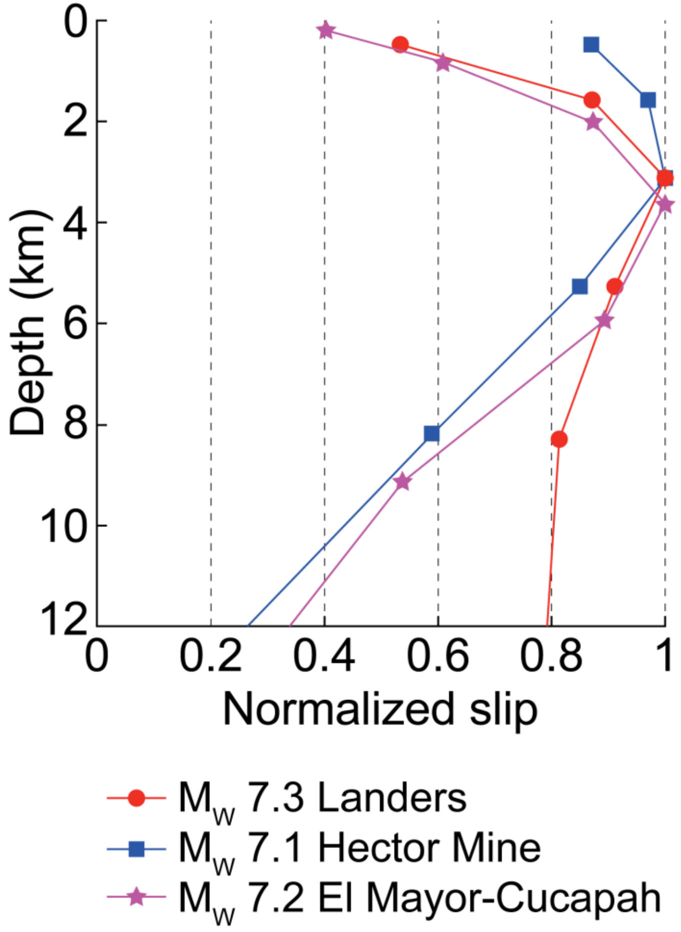

Modified from *Fialko al.* [2005]

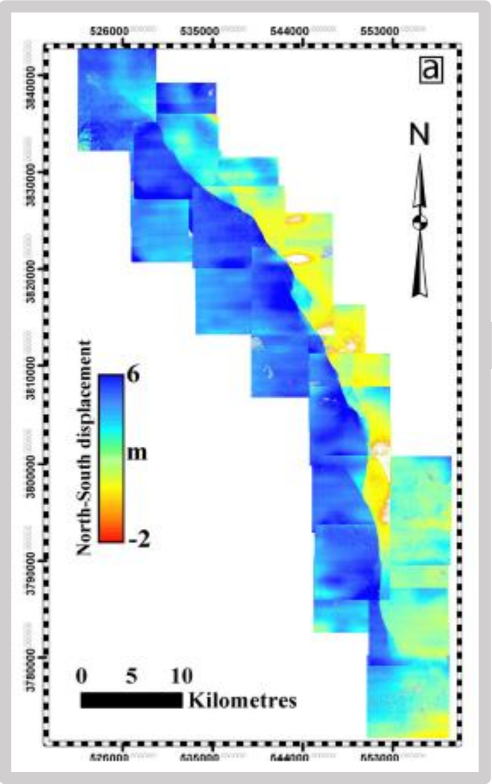

NEAR-FIELD DATA

SSD = 3-19%

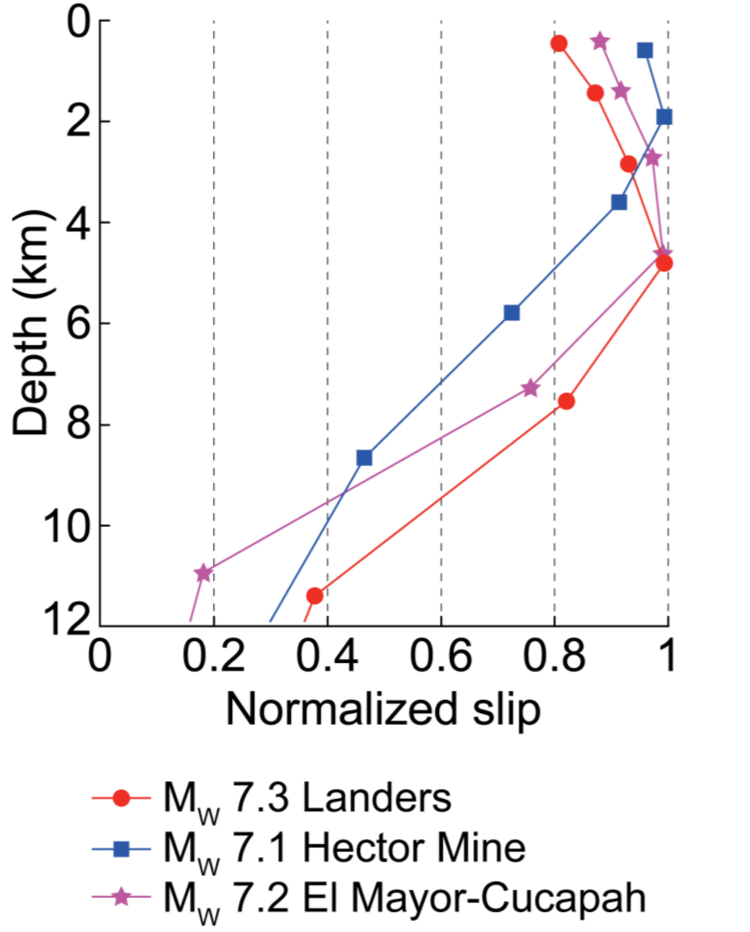

Modified from *Xu et al.* [2016]

2. How sensitive is shallow deformation to constitutive properties?

Hazard Implications:
- Inversion capabilities
- Deformation of shallow infrastructure (e.g., gas, water pipelines)

Compliant Zone Elastic
(e.g., Barbot et al., 2008)

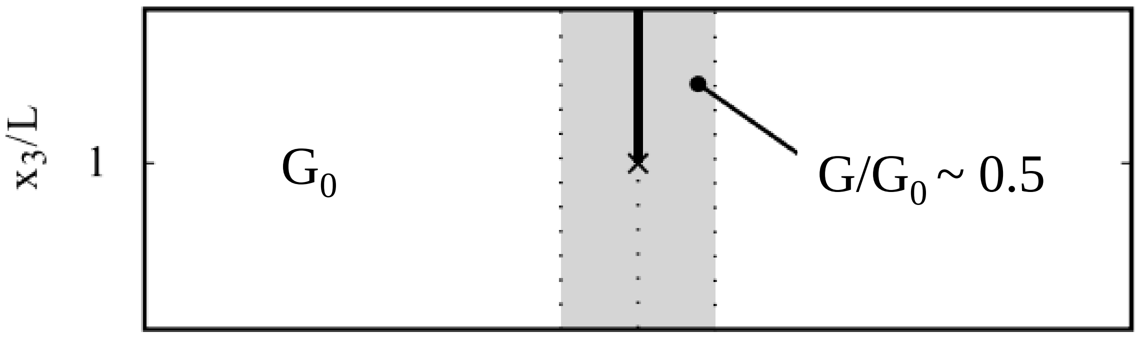

Homogeneous Elastic
(e.g., Okada, 1985)

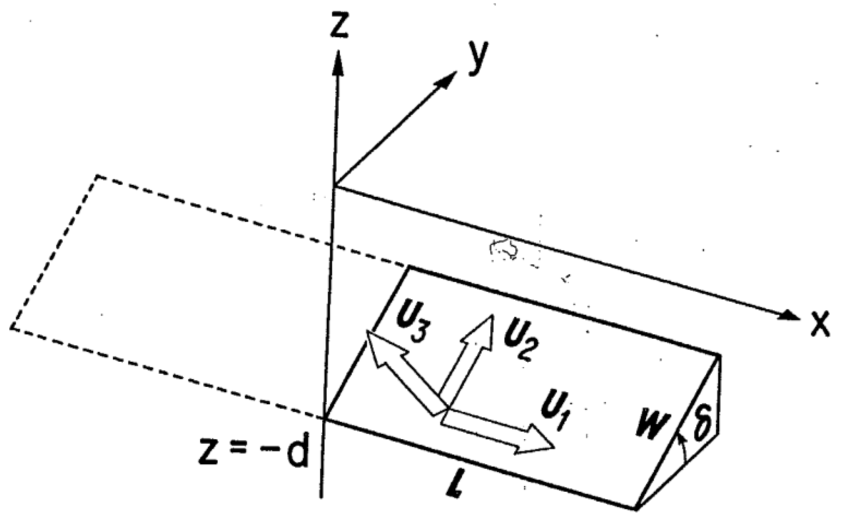

Elastoplastic
(e.g., Kaneko & Fialko, 2011)

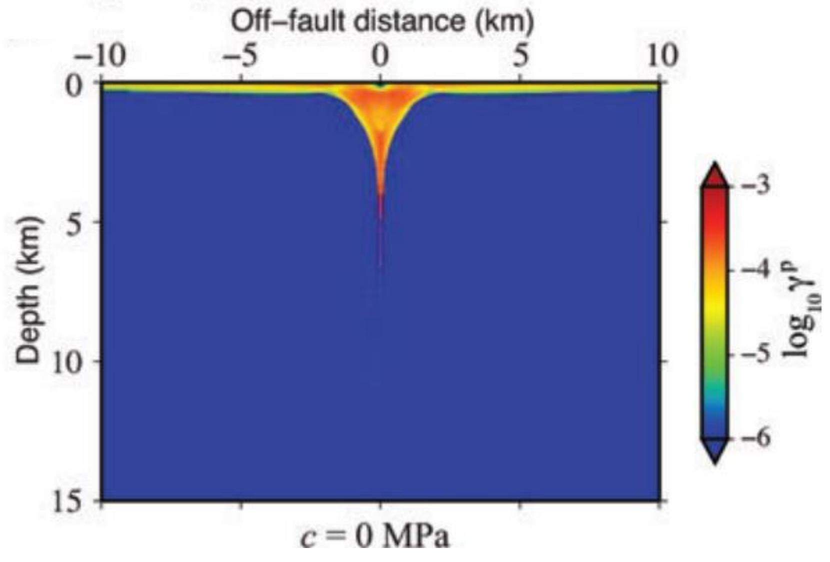

Compliant Zone type example: Punchbowl Fault

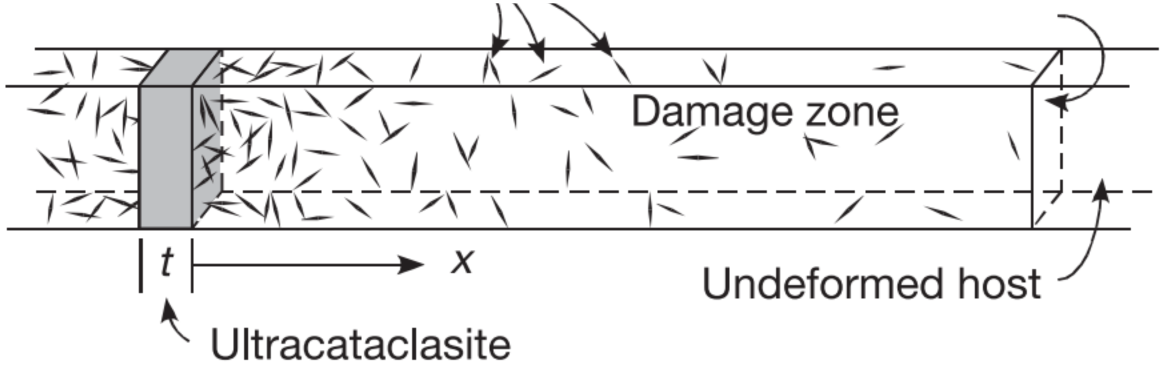

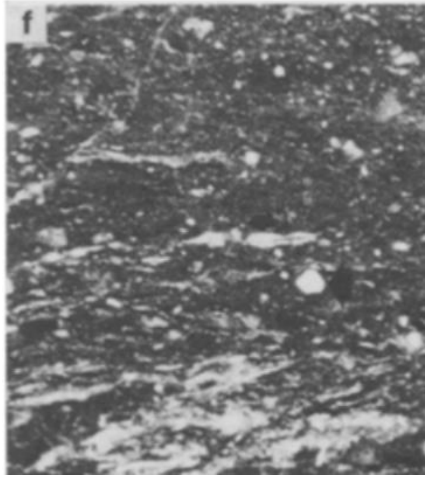

Fault core

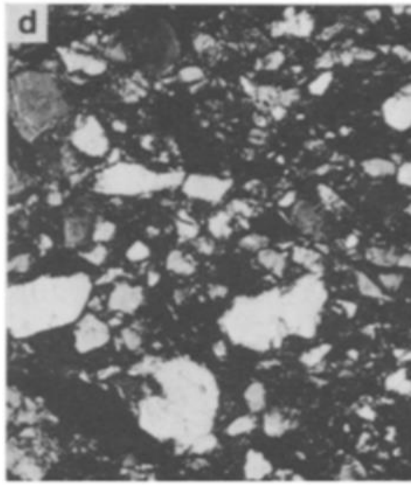

Damage Zone

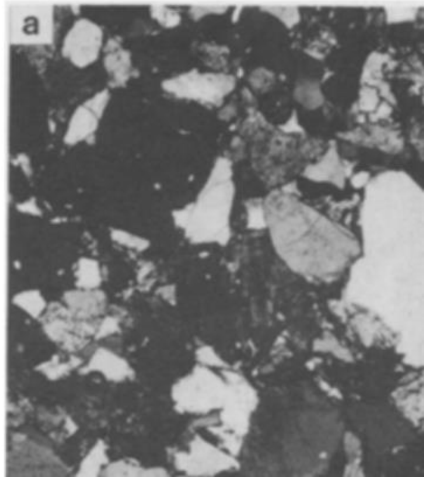

Undeformed

[*Chester & Logan,* 1986; *Chester et al.*, 2005]

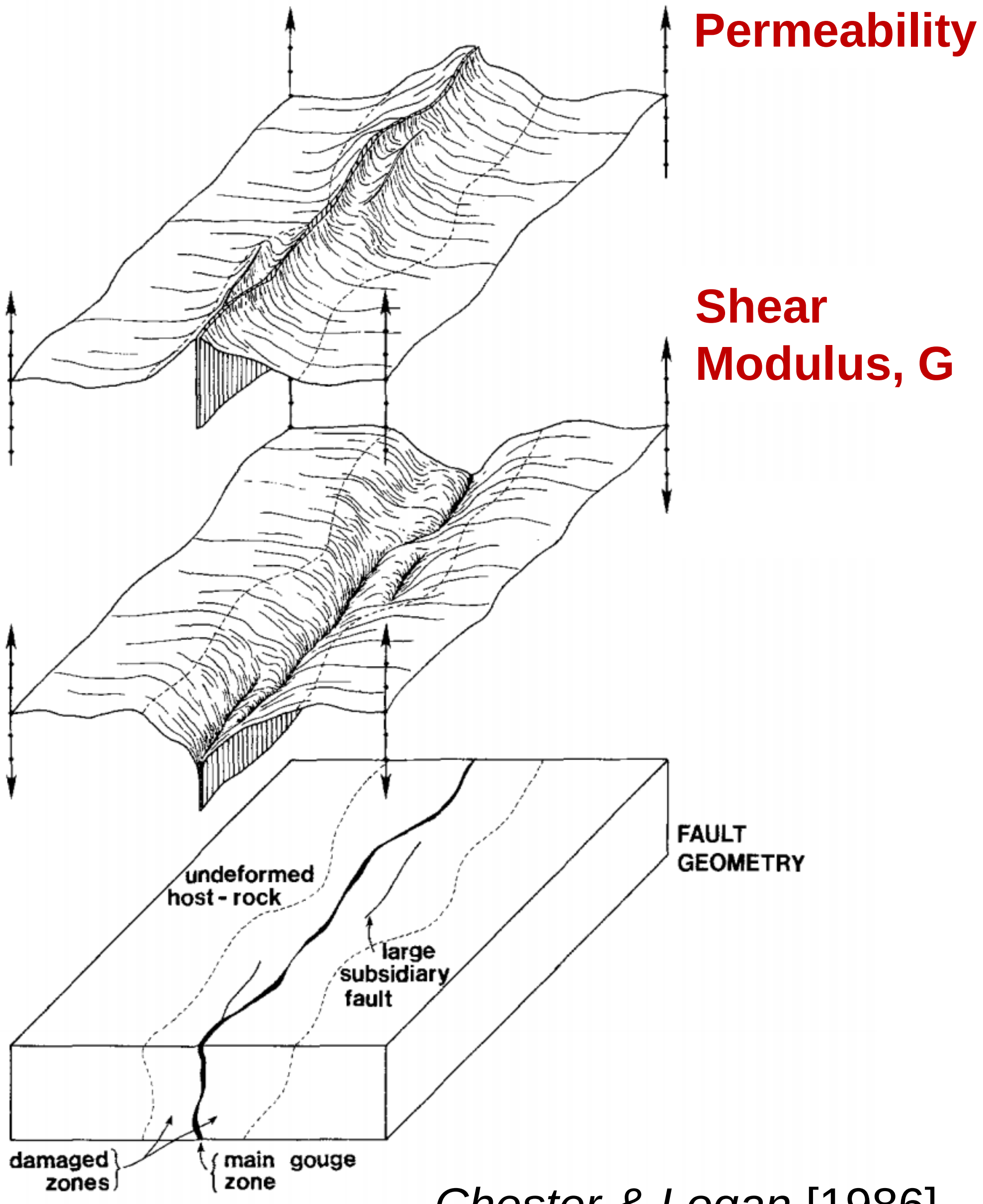

Chester & Logan [1986]

Compliant Zones: Geodetic and seismological evidence

1999 **M** 7.1 Hector Mine EQ

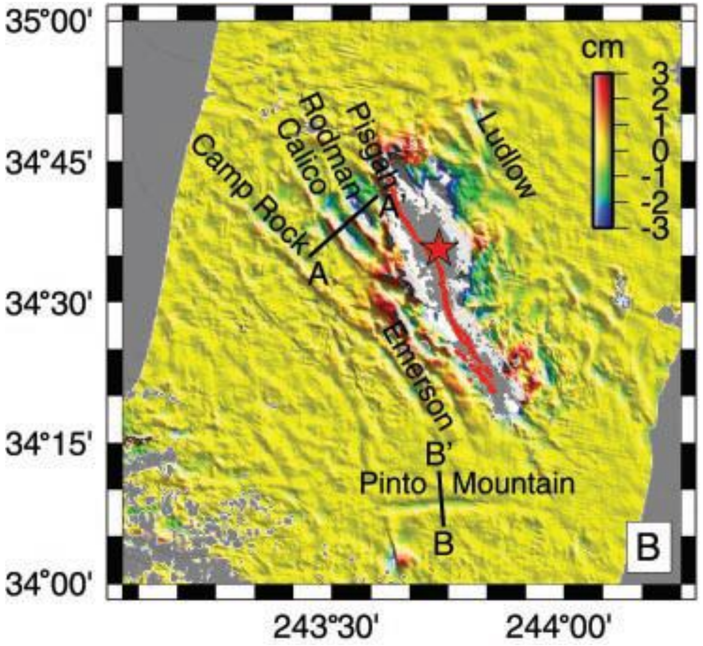

Fialko et al. [2002]

Surface deformation (InSAR)

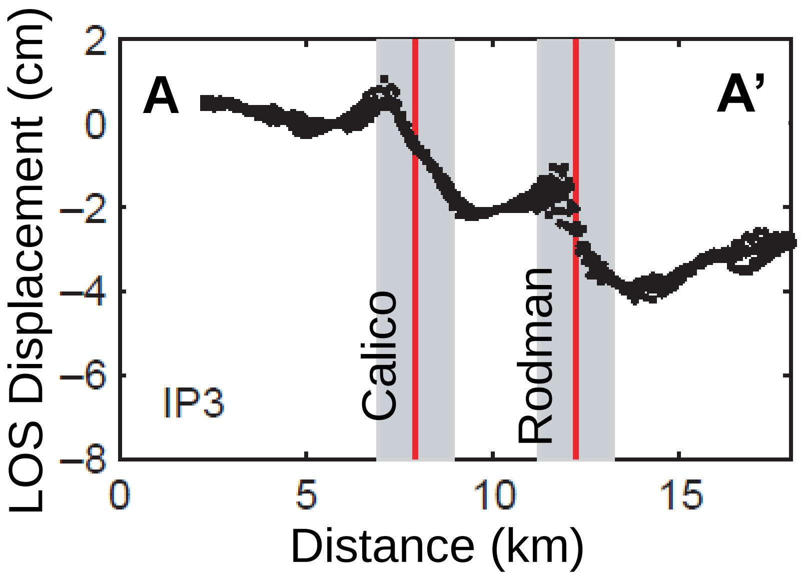

Trapped waves in Calico Fault

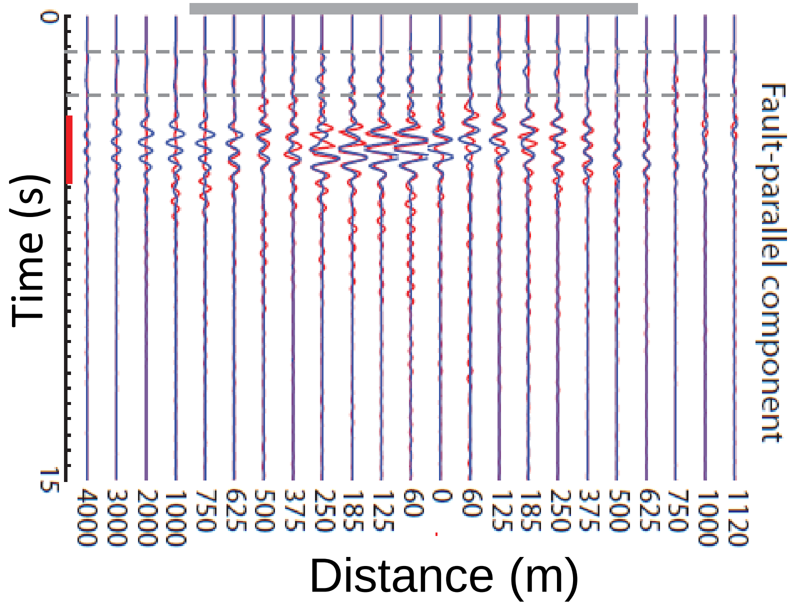

Cochran et al [2009]

Surface deformation confined to compliant zones during remote loading

What happens when the fault within the CZ slips?

Plastic Deformation: Geodetic and field evidence

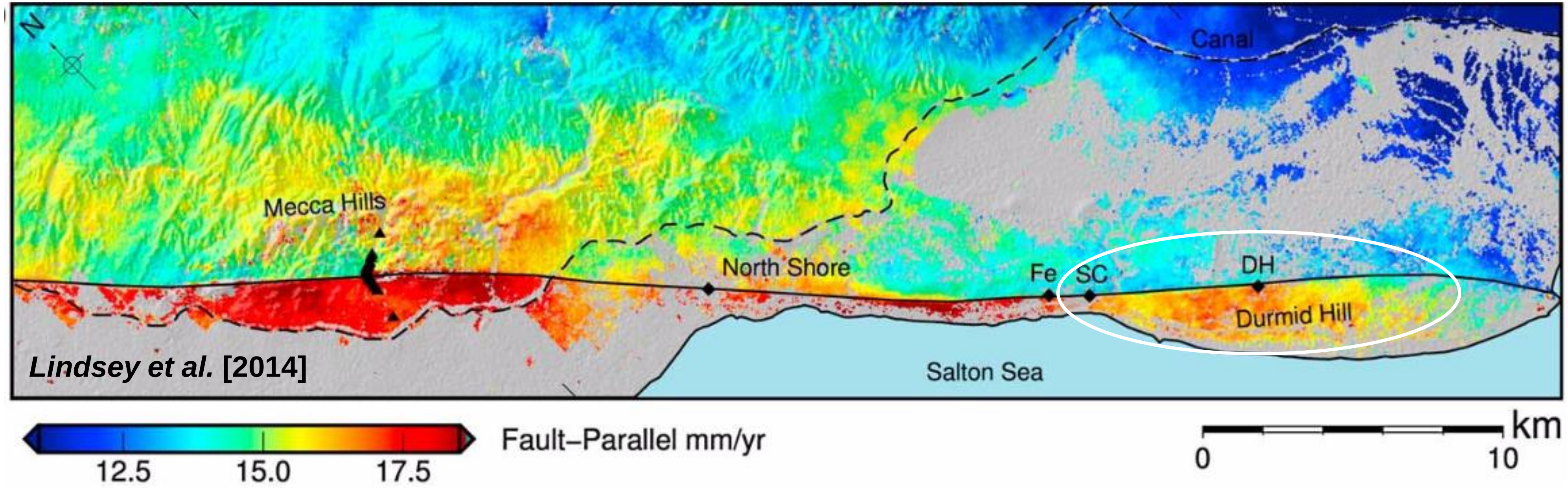

InSAR shows distributed deformation across San Andreas near Durmid Hill

No evidence of km-scale compliant zone

Plastic Deformation: Geodetic and field evidence

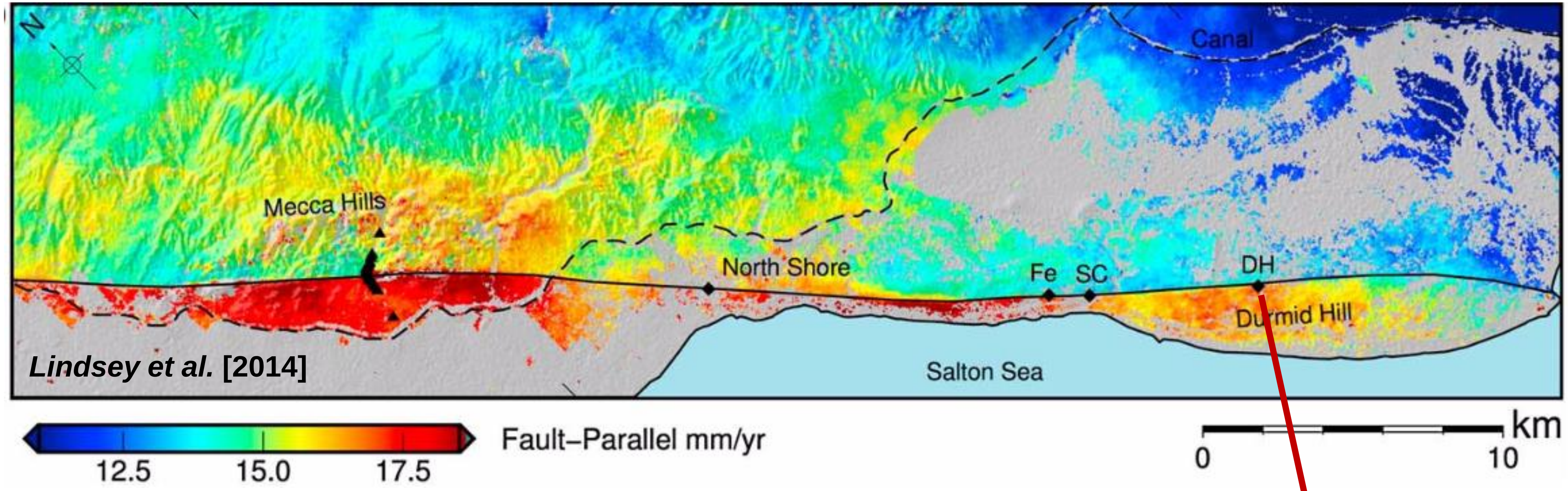

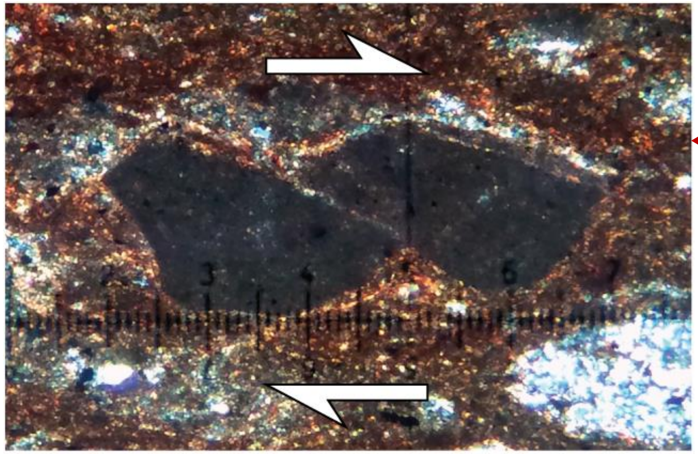

500 µm

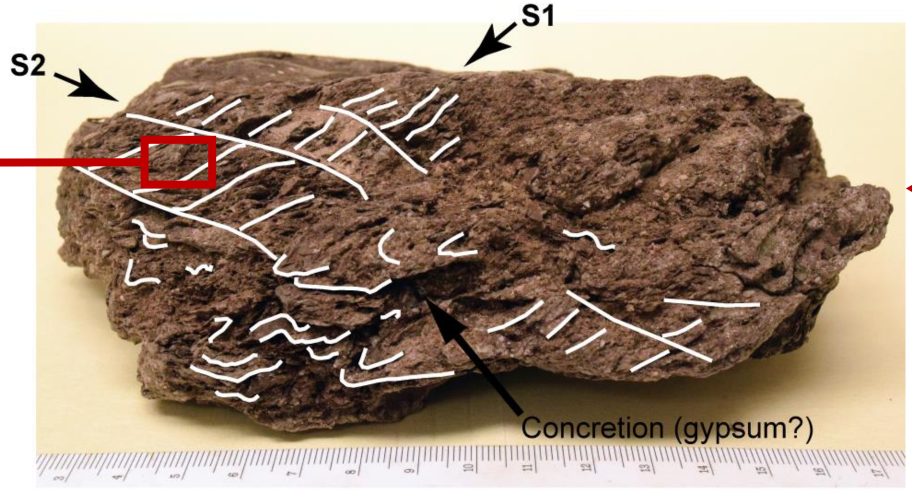

5 cm

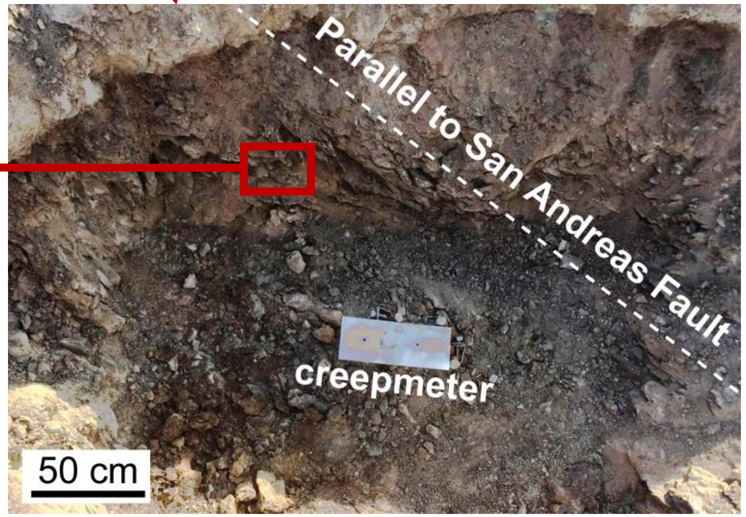

Photo and sample courtesy of Roger Bilham

2. How sensitive is shallow deformation to constitutive properties?

Hazard Implications:
- Inversion capabilities
- Deformation of shallow infrastructure (e.g., gas, water pipelines)

Compliant Zone Elastic
(e.g., Barbot et al., 2008)

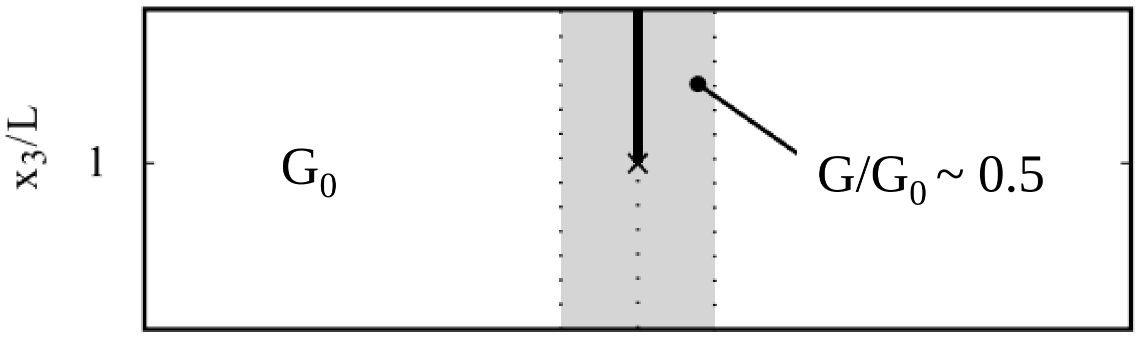

Homogeneous Elastic
(e.g., Okada, 1985)

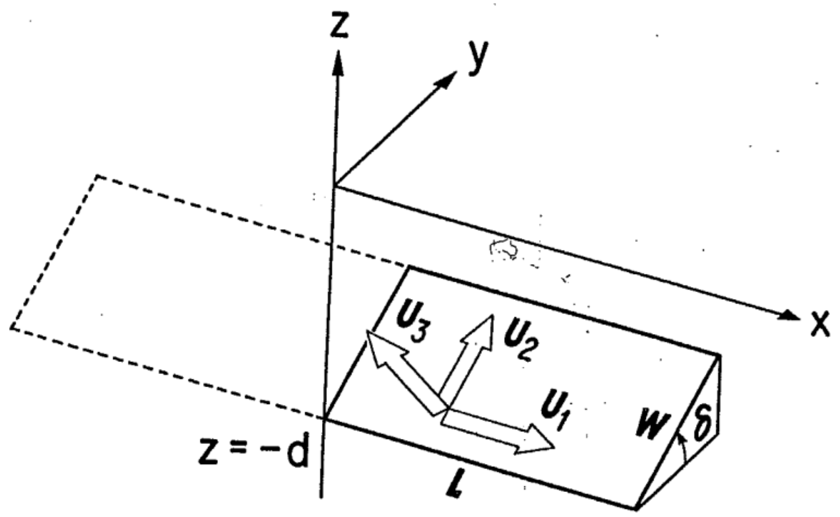

Elastoplastic
(e.g., Kaneko & Fialko, 2011)

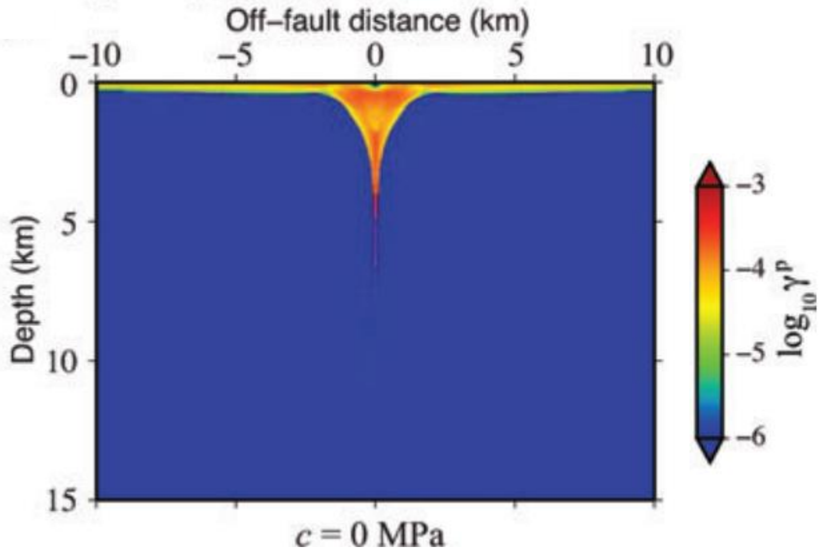

3. Can surface deformation reveal rupture dynamics?

Bulletin of the Seismological Society of America, Vol. 98, No. 4, pp. 1609–1632, August 2008, doi: 10.1785/0120070111

Displacement and Geometrical Characteristics of Earthquake Surface Ruptures: Issues and Implications for Seismic-Hazard Analysis and the Process of Earthquake Rupture

by Steven G. Wesnousky

Table 1
Geological Observations

Date (mm/dd/yyyy)	Location	Number	Type*	Length (km)‡	$S^{†}$ (Average Net Slip) (m)	S^{max} Max Slip (m)	Depth (km)	Rigidity μ (10^{11} dyne cm^{-2})	M_0^G (10^{26} dyne cm)	P_0^G (10^{15} cm^3)	M_w^G	Reference§	Notes‖
01/09/1857	San Andreas, CA	1	SSR	360	4.7	9.1 (12)	15	3	76	25.4	7.9	1	a
05/03/1887	Sonora, MX	2	N/60	70	2.2	4.1	15	3	8.0	2.7	7.2	2, 3, 48	b
10/28/1891	Neo-Dani, Japan	3	SSL	80	3.1	7.9	15	3	11.3	3.8	7.3	4	c
08/31/1896	Rikuu, Japan	4	R/45	37	2.5 (3.5)	6.2 (8.8)	15	3.0	8.2	2.7	7.2	5	d
10/02/1915	Pleasant Valley, NV	5	N/45	61	1.8 (2.6)	5.8 (8.2)	15	3.1	10.3	3.4	7.3	6	e
11/02/1930	Kita-Izu, Japan	6	SSL	35	1.1	3.5	12	3.3	1.6	0.48	6.7	7	f
12/25/1939	Erzincan, Turkey	7	SSR	300	4.2	7.4	13	3.2	52.5	16.4	7.7	8	g
05/19/1940	Imperial, CA	8	SSR	60	1.6	3.3	13	2.5	3.0	1.2	6.9	9	h
12/20/1942	Erbaa-Niksar, Turkey	9	SSR	28	1.66	1.9	13	3.2	1.8	0.6	6.8	8	I
11/26/1943	Tosya, Turkey	10	SSR	275	2.5	4.4	13	3.2	28.7	9.0	7.6	8	j
09/10/1943	Tottori, Japan	11	SSL	10.5	0.6	1.5	15	3.3	0.3	0.09	6.3	10	k
02/01/1944	Gerede-Bolu, Turkey	[illegible]	[illegible]	155	2.1	[illegible]	13	3.2	[illegible]	[illegible]	7.35	8	l
01/31/1945	Mikawa, Japan	[illegible]	[illegible]	4.0	1.3	[illegible]	8	[illegible]	[illegible]	.08	6.2	11	m
12/16/1954	Fairview Peak, NV	[illegible]	NSSR/60	62	1.1	[illegible]	[illegible]	3.0	[illegible]	1.2	7.0	13	n
12/16/1954	Dixie Valley, NV	16	N/60	47	0.8 (0.9)	3.1 (3.5)	12	3.0	1.76	0.6	6.8	13	t
08/18/1959	Hebgen Lake, MT	14	N/50	25	2.5	5.4	15	3.0	3.7	1.25	7.0	12	s
07/22/1967	Mudurnu, Turkey	17	SSR	60	0.9	2.0	12	2.4	1.6	0.65	6.7	8	u
04/08/1968	Borrego Mtn, CA	[illegible]	[illegible]	[illegible]	[illegible]	[illegible]	[illegible]	[illegible]	[illegible]	[illegible]	[illegible]	14	v
02/09/1971	San Fernando, CA	[illegible]	[illegible]	[illegible]	[illegible]	[illegible]	[illegible]	[illegible]	[illegible]	[illegible]	[illegible]	59	ap
06/02/1979	Cadoux, Australia	20	R/35	10	0.6	1.2	6	3.2	0.20	0.06	6.1	49	x
10/15/1979	Imperial Valley, CA	21	SSR	36	0.28–0.41	0.6–0.78	13	2.5	0.33–0.48	0.13–0.19	6.3–6.4	15, 16	w
10/10/1980	El Asnam, Algeria	[illegible]	[illegible]	27.3	[illegible]	6.5	12	3.0	[illegible]	[illegible]	6.7	60	aq
07/29/1981	Sirch, Iran	[illegible]	[illegible]	[illegible]	[illegible]	[illegible]	15	[illegible]	[illegible]	[illegible]	[illegible]	50	aj
10/28/1983	Borah Peak, ID	[illegible]	[illegible]	[illegible]	[illegible]	[illegible]	[illegible]	[illegible]	[illegible]	0.89	6.9	17	y
03/03/1986	Marryat, Australia	25	R/35	13	0.24 (sec) (0.42) 0.26*u* (0.46)	0.70 (sec) (1.2) 0.8*u* (1.4)	3	3.2	0.09 (sec) 0.10*u*	0.03 (sec) 0.03*u*	[illegible] (sec) 5.9*u*	46	z
03/02/1987	Edgecumbe, NZ	27	N/60	15.5	0.6 (0.7)	2.6 (3.0)	10	2.6	0.33	0.13	6.3	19	ao
11/23/1987	Super. Hills, CA	26	SSR	25	0.3–0.6	0.5–1.1	12	2.5	0.22–0.47	.09–.19	6.2–6.4	18	aa
01/22/1988	Tennant Crk, Australia	28	R/45	30	0.7 (1.0)	1.8 (2.5)	8	3.3	1.1	0.34	6.6	43	ab
07/16/1990	Luzon, Philippines	29	SSL	112	3.5	6.2	20	3.5	27.4	7.84	7.6	20, 21	am
06/28/1992	Landers, CA	30	SSR	77	2.3	6.7	15	3.0	8.1	2.7	7.2	22	ac
03/14/1998	Fandoqa, Iran	31	SSN/54	25	1.1	3.1	10	3.3	1.2	0.36	6.6	50	ag
08/17/1999	Izmit, Turkey	34	SSR	107 (145)	1.1	5.1	13	3.2	4.9	1.5	7.1	47	ae
09/21/1999	Chi-Chi, Taiwan	32	R/70	72	3.5 (4.0)	12.7 (16.4)	20	3.0	18.4	6.1	7.4	23	ad
10/16/1999	Hector Mine, CA	33	SSR	44	1.56	5.2	12	3.0	2.5	0.82	6.9	57	an
11/12/1999	Duzce, Turkey	35	SSR	40	2.1	5.0	13	3.2	3.5	1.1	7.0	24	af
11/14/2001	Kunlun, China	36	SSL	421	3.3	8.7	15	3.0	62.5	20.8	7.8	53	am
11/14/2001 (spot)	Kunlun, China	36a	SSL	428	2.4	8.3	15	3.0	46.8	15.6.	7.8	61	al
11/03/2002	Denali, AK	37	SSR	302	3.6	8.9	15	3.2	51.6	16.1	7.7	52	ak

*Type of earthquake mechanism and dip. Right- and left-lateral strike slip are SSR and SSL, respectively. Reverse and normal events are R and N, respectively. Right-lateral normal oblique motion is NSSR.
†See column labeled Notes for an explanation of the calculation for each event. When two values are given, the value in rounded brackets is the calculated net slip and the other is for the type of slip provided in the original slip distribution.
‡The digitized distance along fault rupture trace.
§See Table 3 for the key to the references.
‖See Ⓔ the electronic edition of *BSSA* for notes bearing on the basis for assigning column values and location of the epicenter when plotted.

Of 31 studies, only 7 reported observations within 24 hours of EQ

Hayward Fault simulations suggest 40% afterslip within 24 hrs

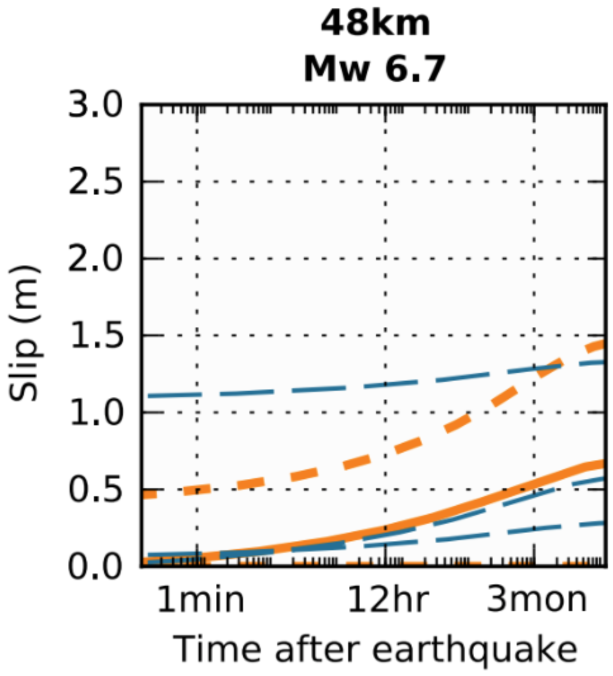

Aagaard et al. [2012]

Hazard Implication:
Empirical relationships based on this data (e.g., GMPEs) may be flawed

2014 **M** 6.0 South Napa Earthquake

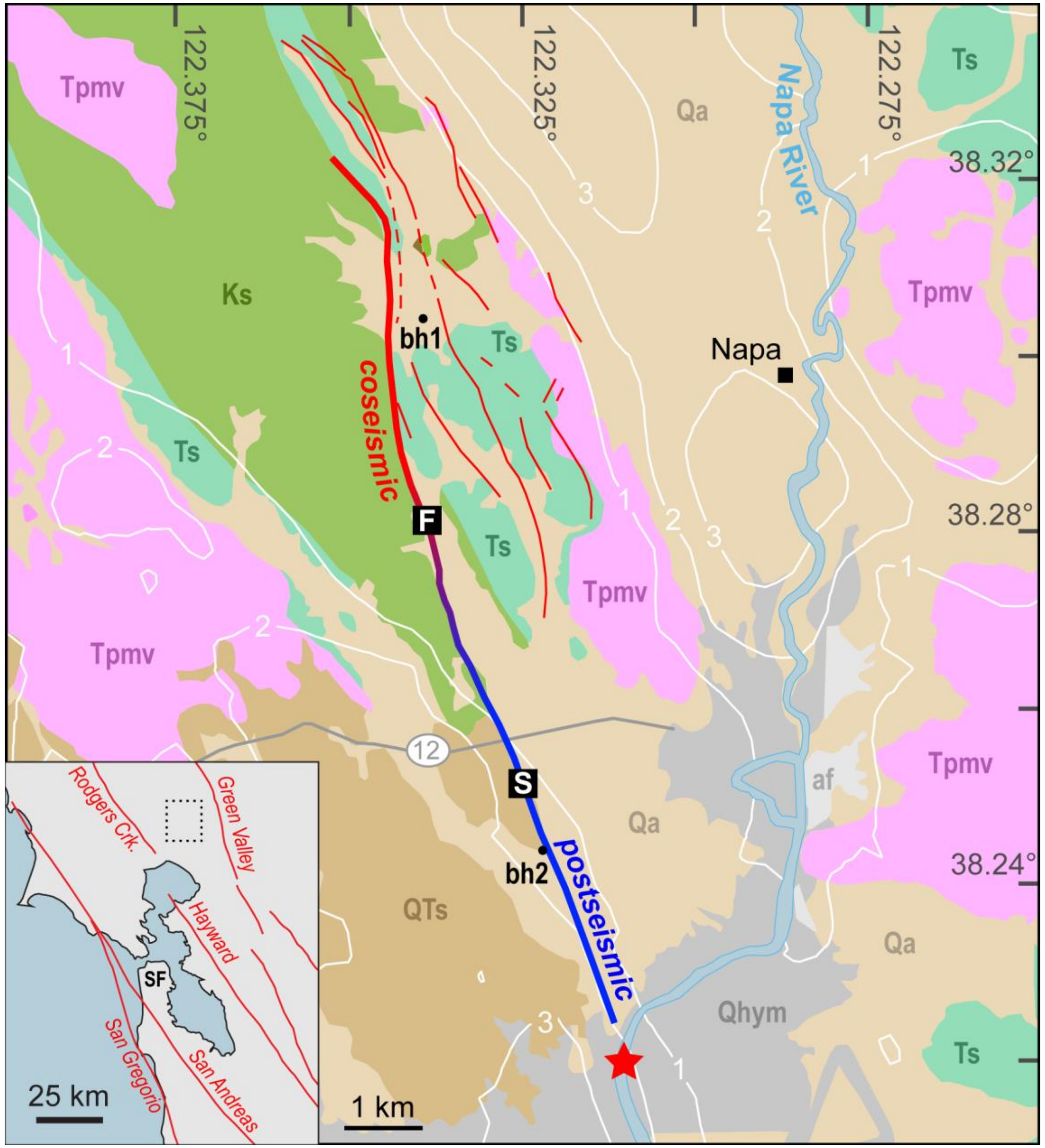

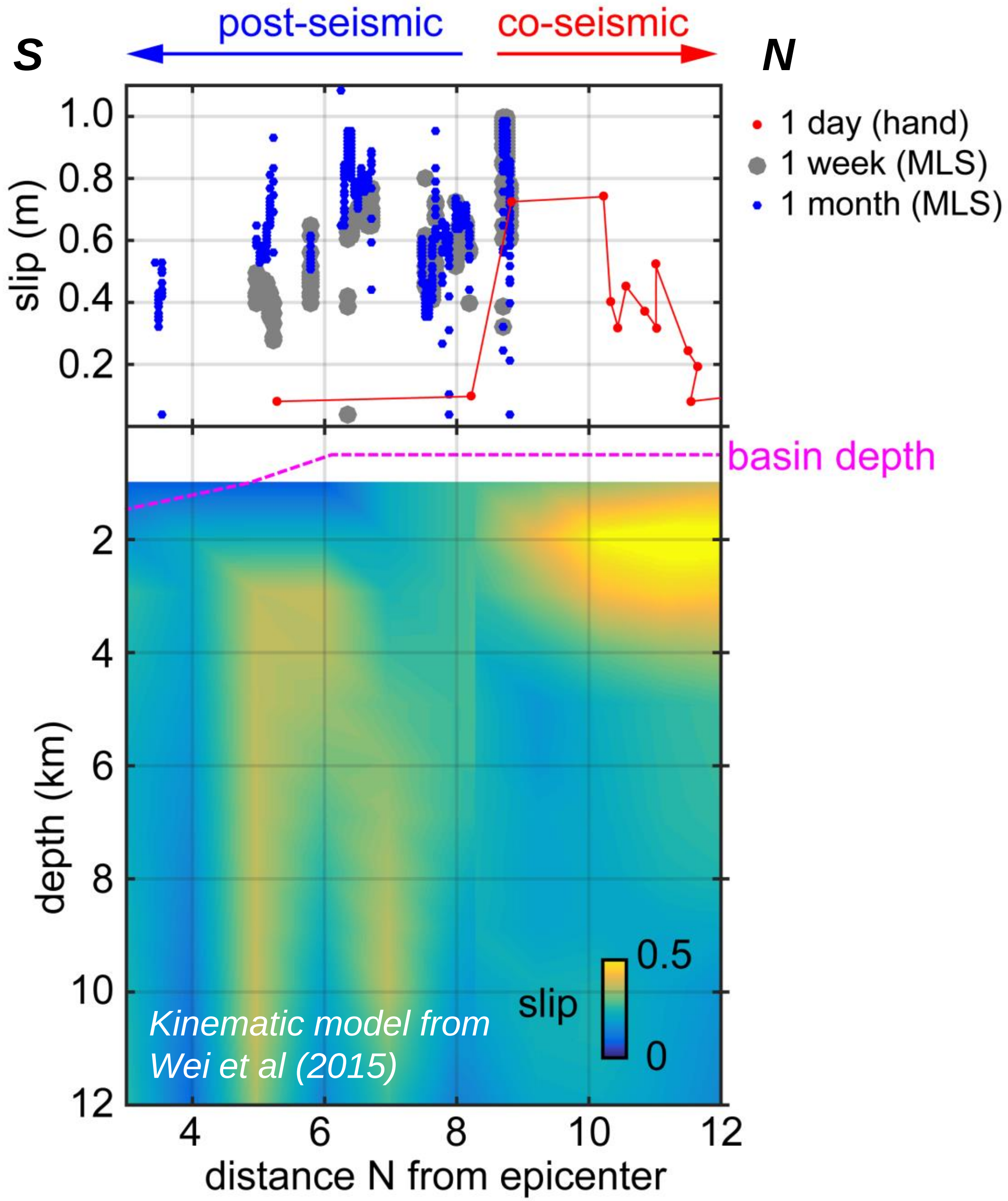

Deflected vine rows record deformation

EERI [2014]

En echelon secondary fractures observed along length of rupture

Hudnut *et al.* [2014]

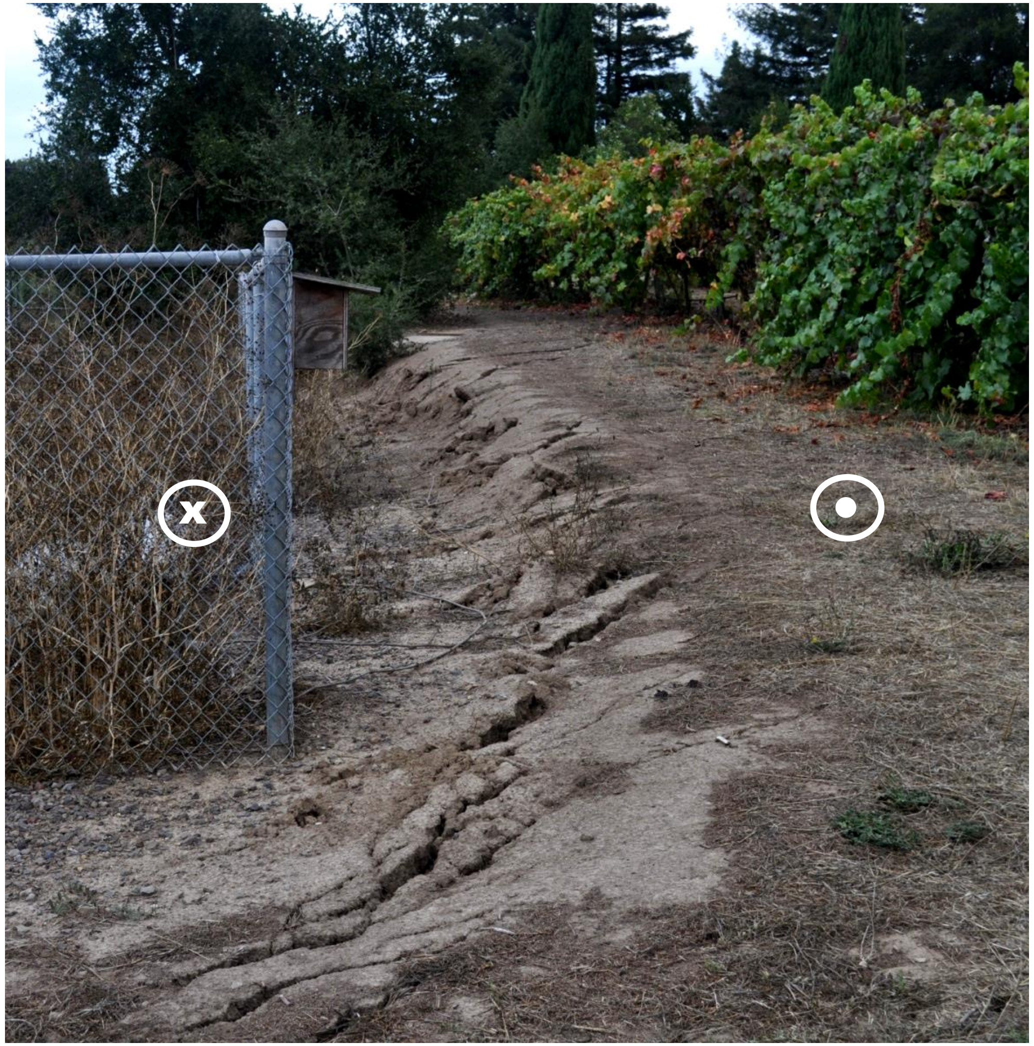

En echelon secondary fractures observed along length of rupture

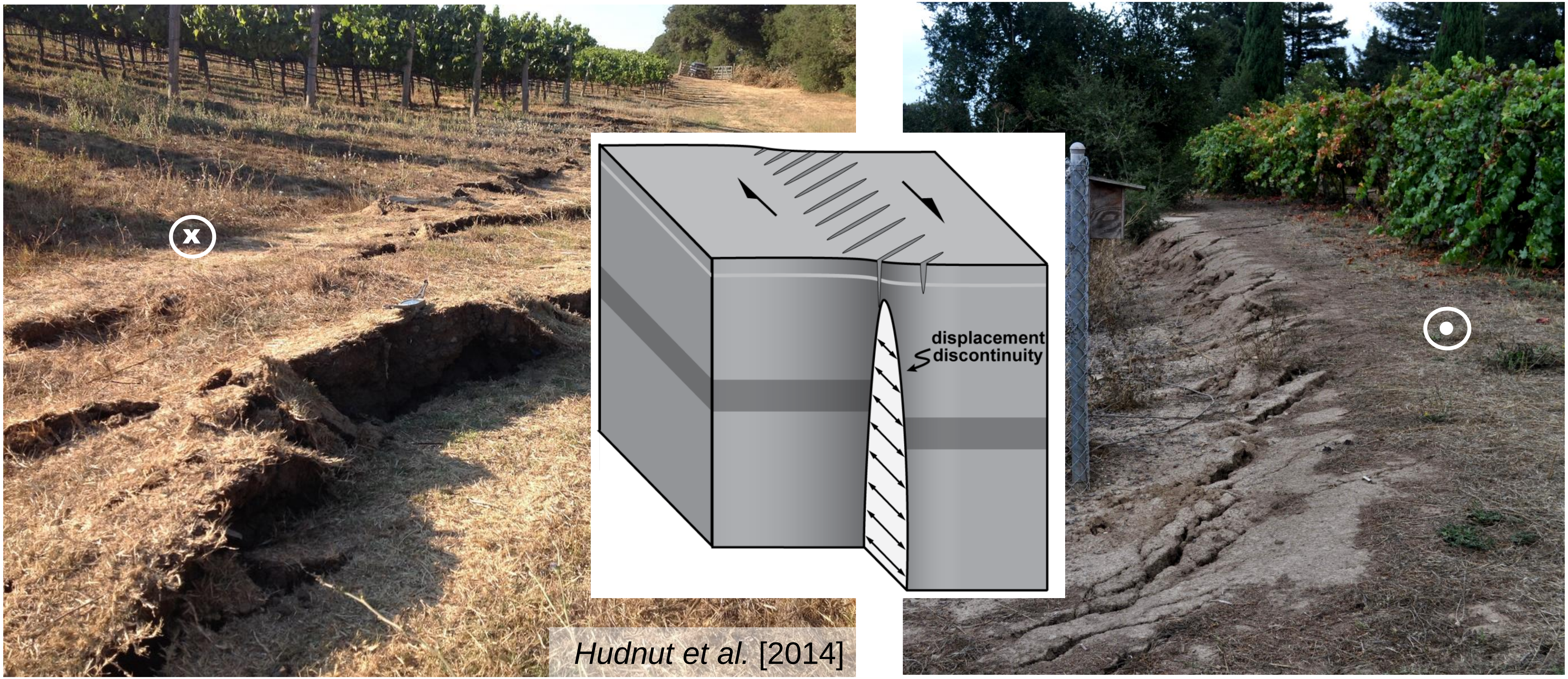

Hudnut et al. [2014]

Trenches confirm buried fault tip and distributed deformation

South Avenue Trench

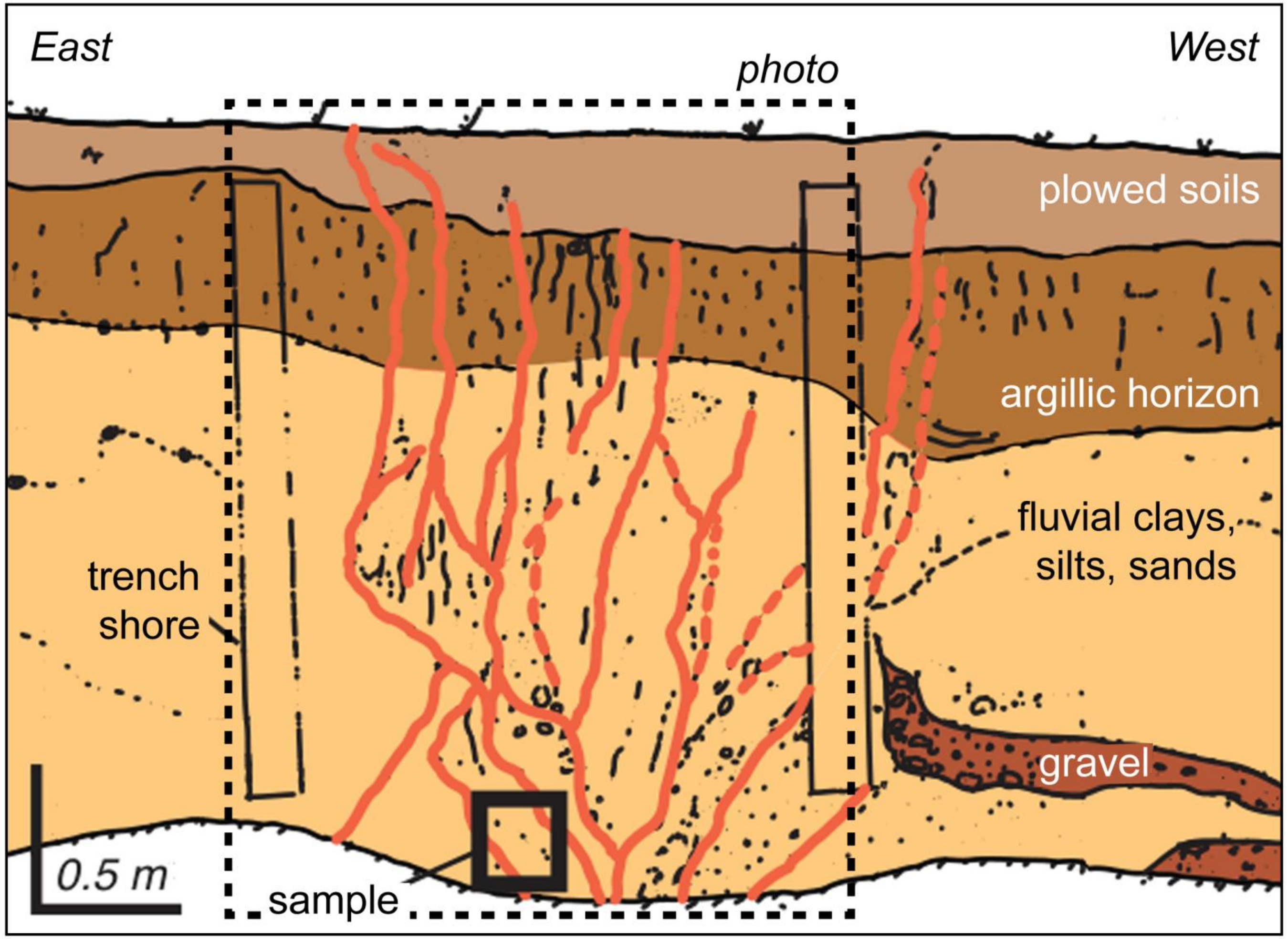

Brooks et al. [accepted]

Courtesy of Tim Dawson

Trenches confirm buried fault tip and distributed deformation

South Avenue Trench

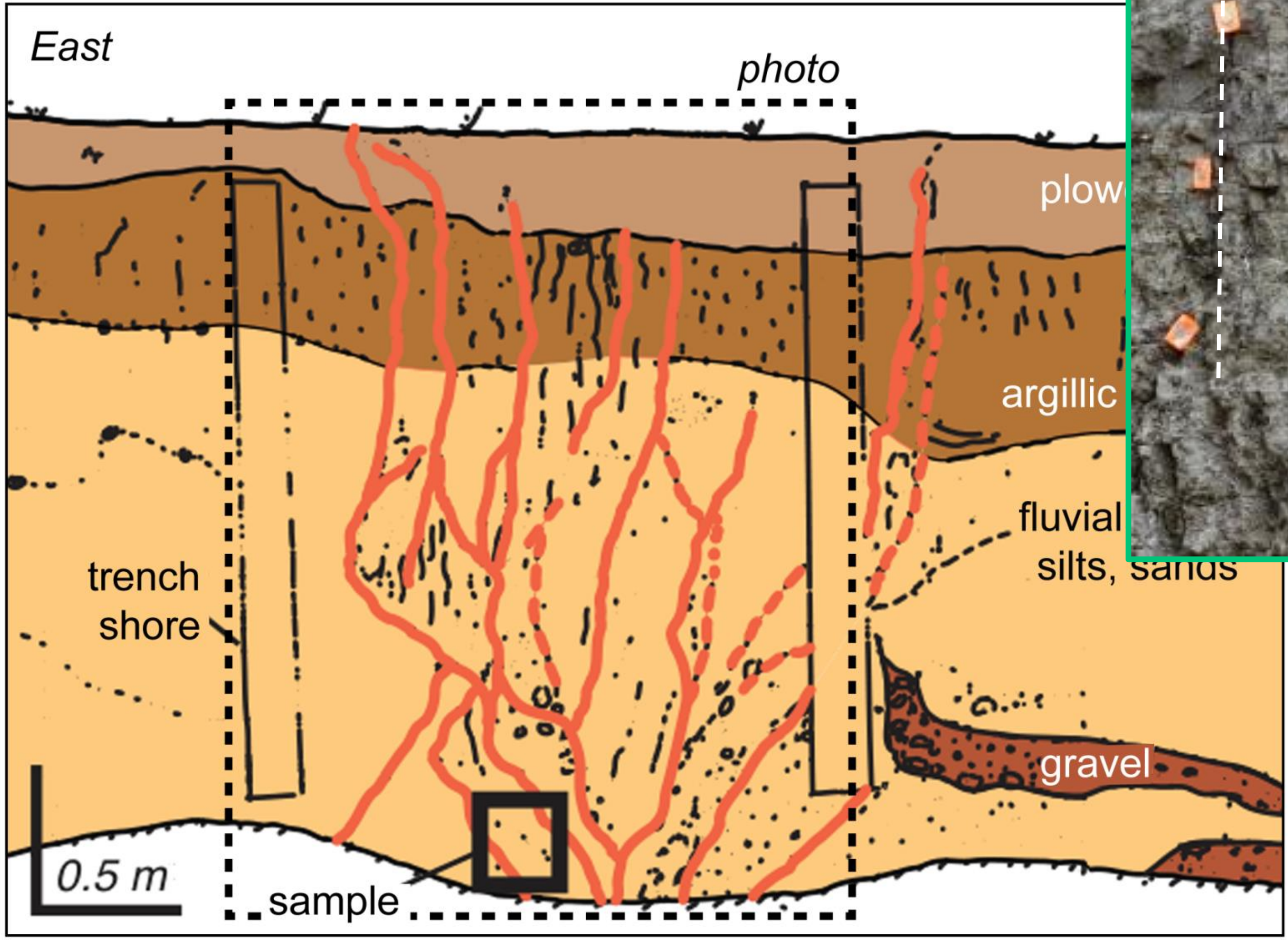

Brooks *et al.* [accepted]

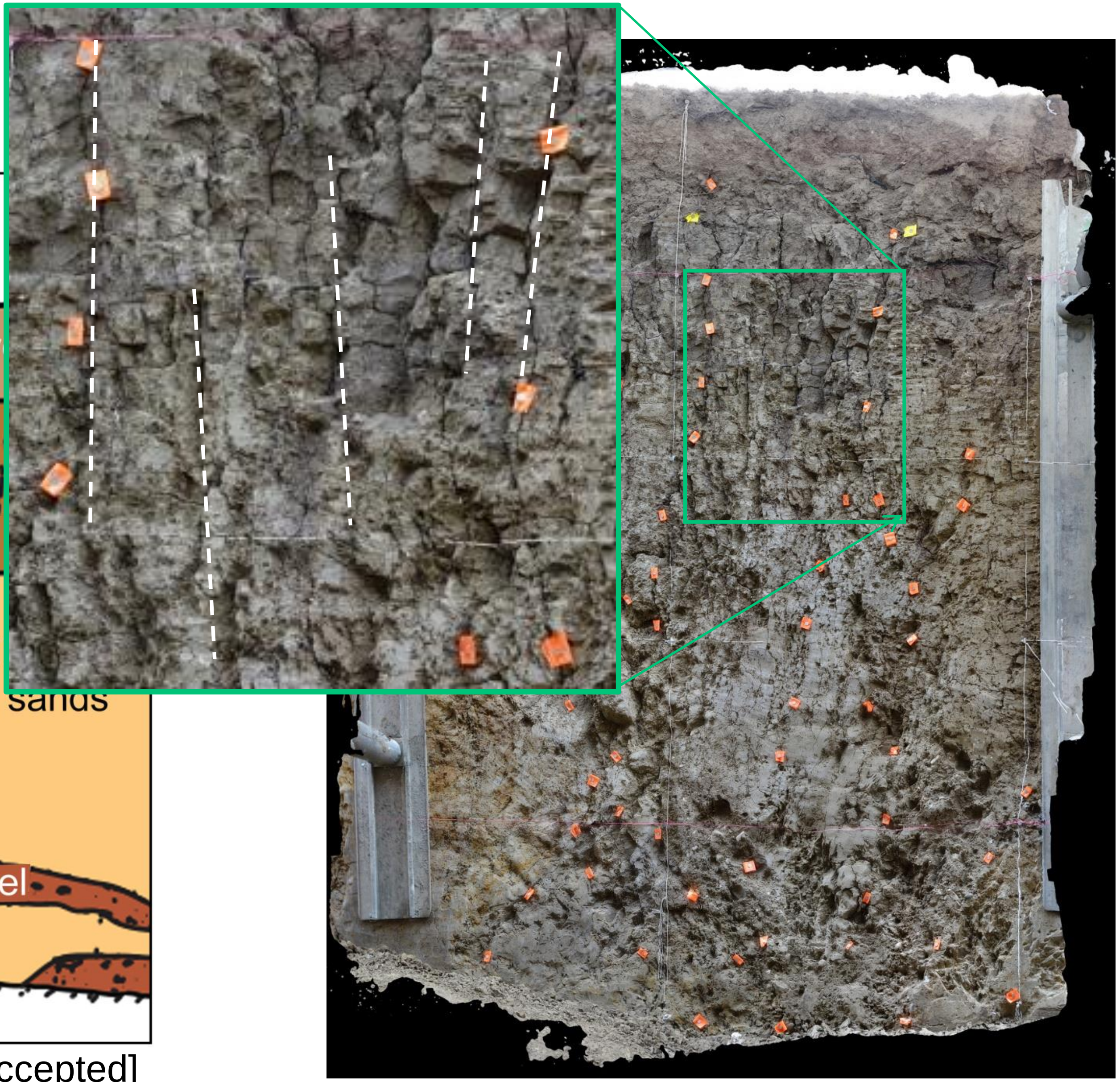

Courtesy of Tim Dawson

Near-field measurements with Mobile Laser Scanning (MLS)

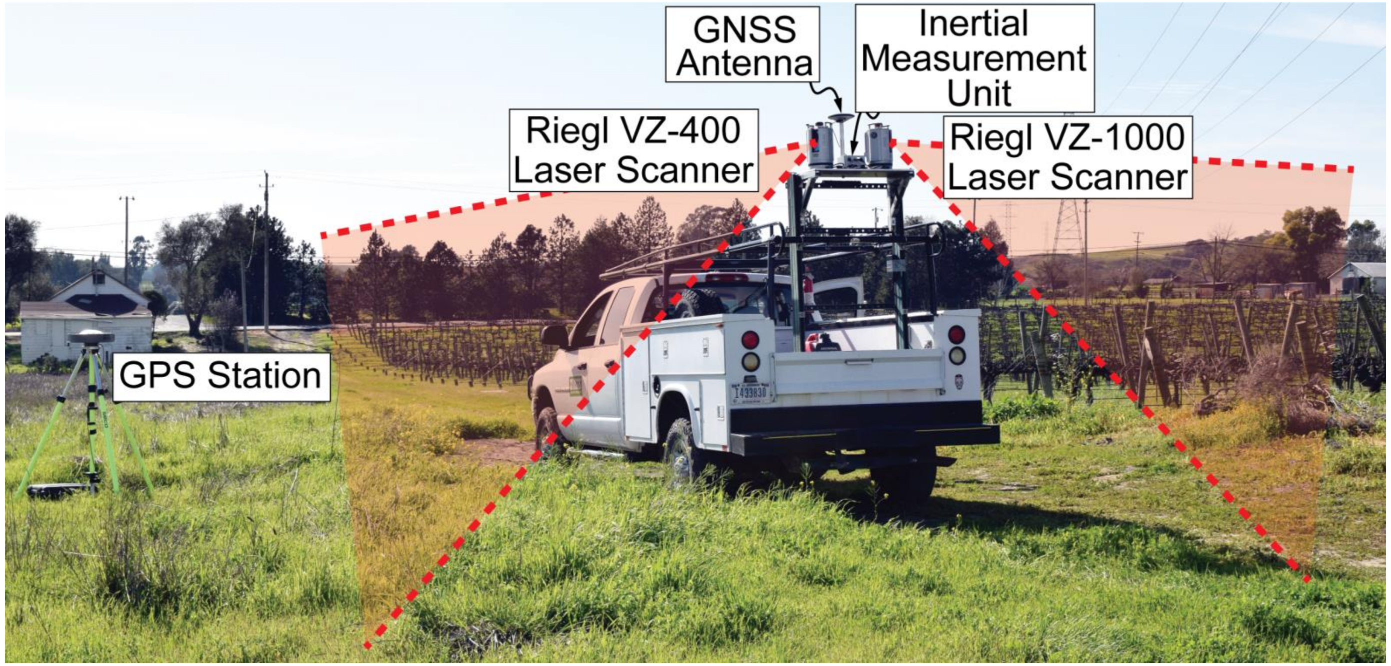

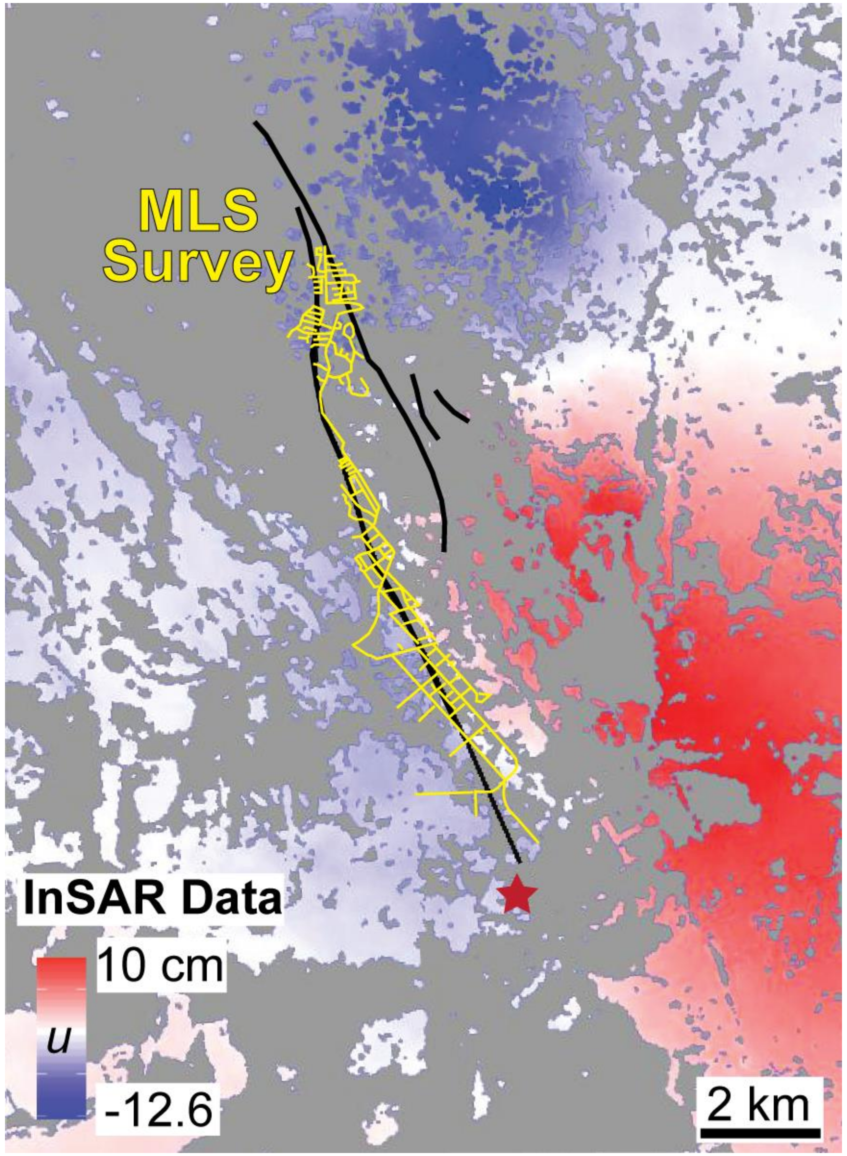

Aria Project

- Covered 80% rupture
- 3 epochs of data: ~1 wk, ~1 mo, ~1 yr
- >5 billion laser reflection points per epoch
- Each point referenced in 3 dimensions
- Accuracy within a few centimeters

Near-field deformation at post- and co-seismic sites

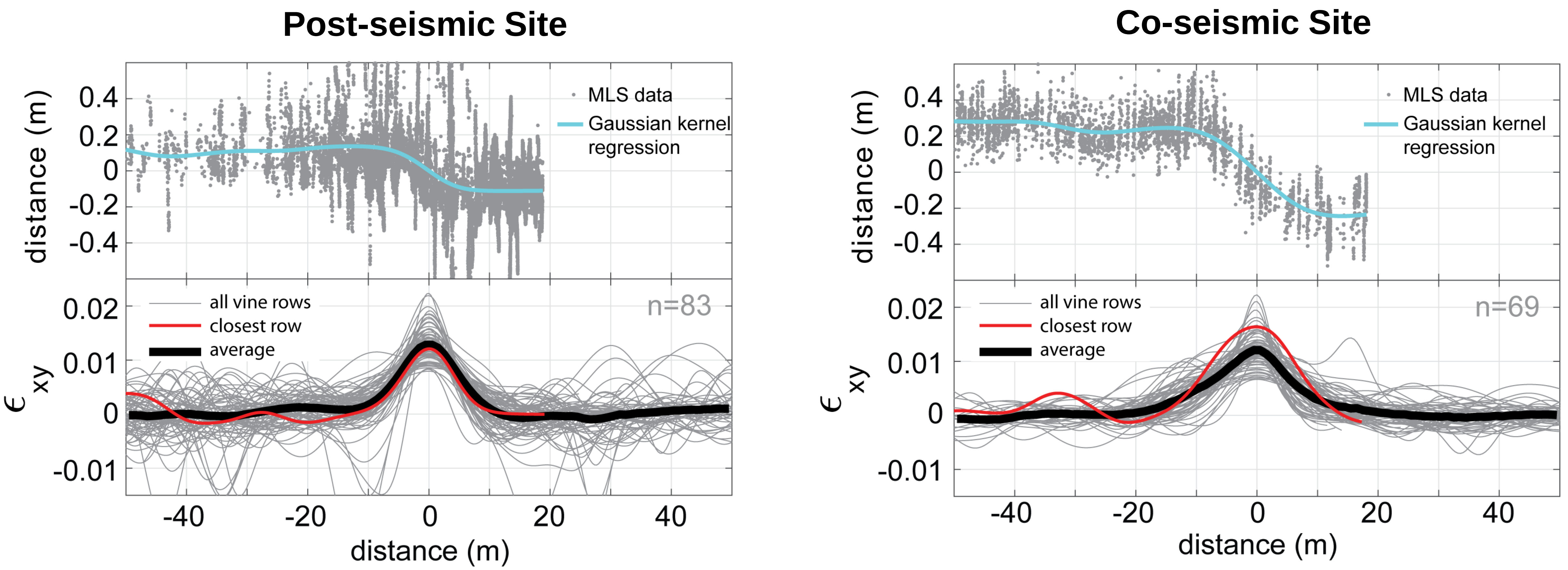

Dynamic slip didn't cause permanent deformation distinguishable from static slip

(i) Neither dynamic nor static stress state met yield criterion, or

(ii) Rupture slowed down such that dynamic terms were negligible

***Bonilla & Lienkaemper* [1990]:**

Examined >1200 fault strands in 163 trenches

70% could *NOT* be traced to the ground surface that existed at the time of faulting.

Trench log for 1906 SF Earthquake:

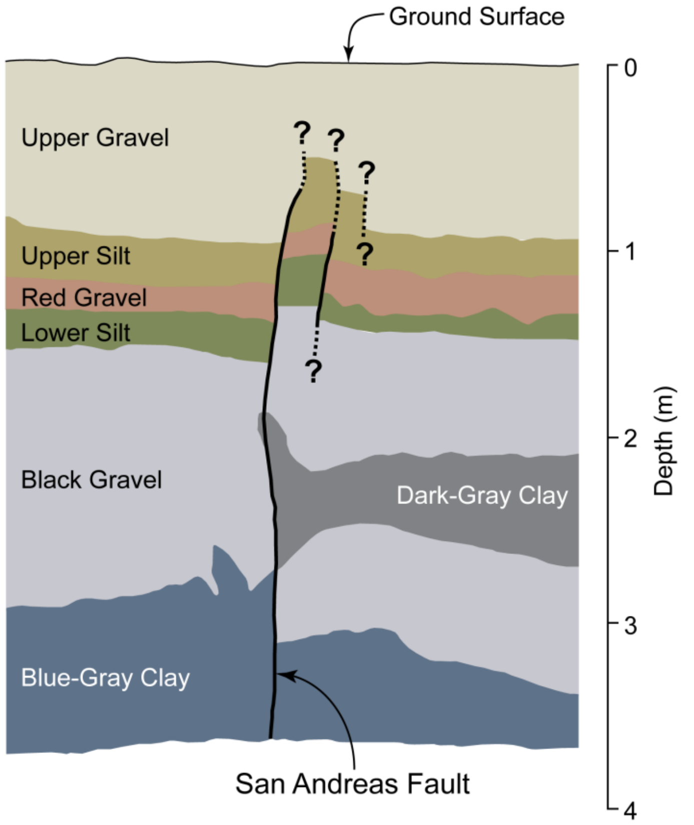

After *Cotton et al.* [1982]

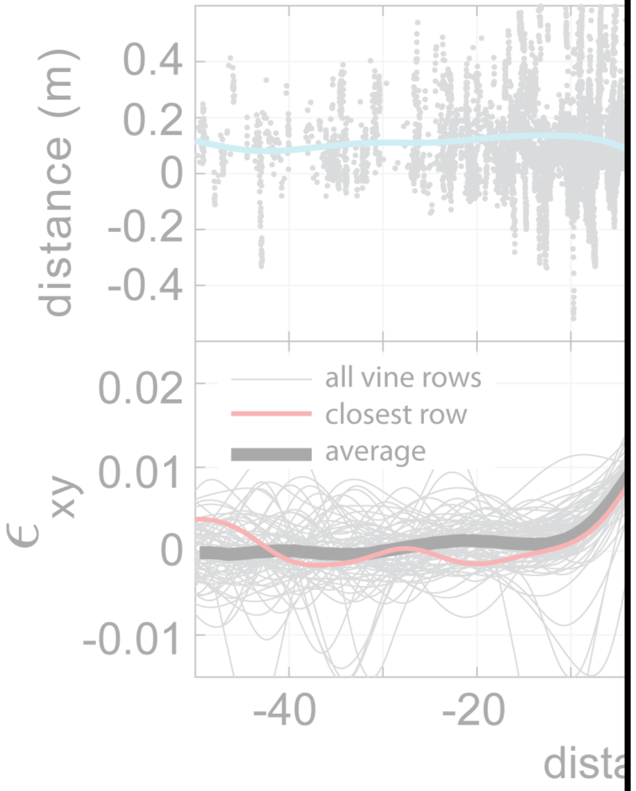

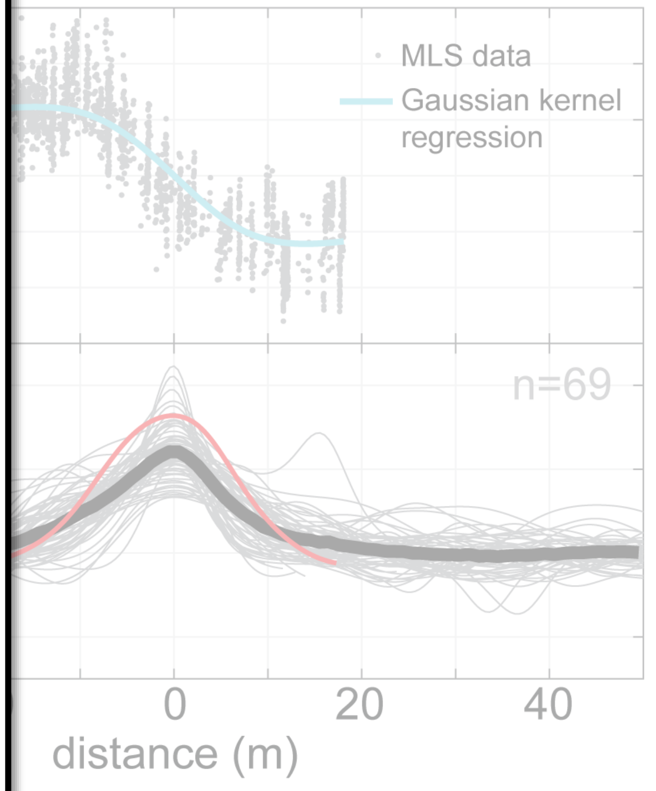

Active-source seismic imaging of shallow subsurface

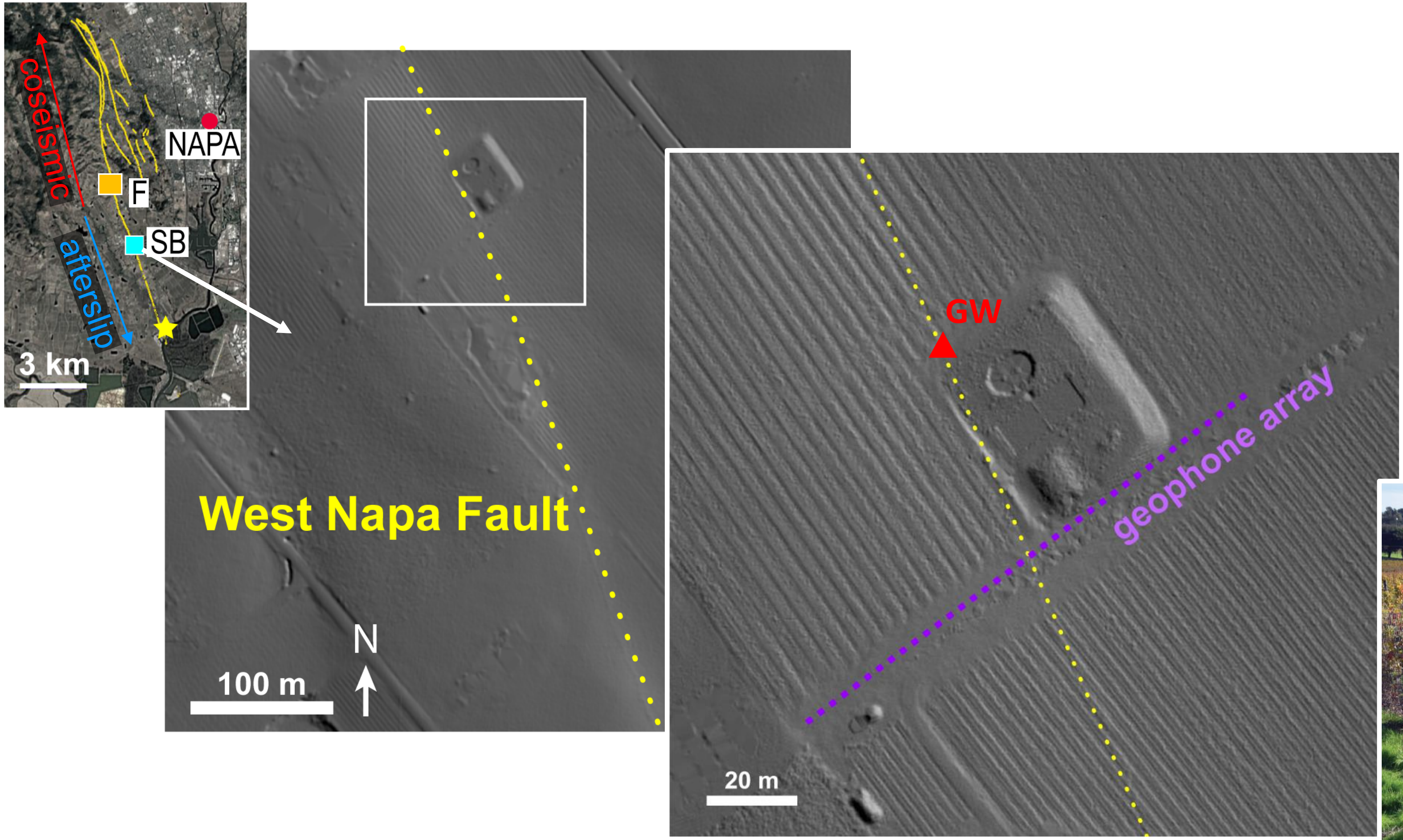

Methodology

- 120 m long survey
- Source/receiver spaced every 1 m
- Active source using hammer and steel plate
- Recorded both P- and S-waves
- Guided waves (GW)

For detailed overview of methodology: Catchings et al., BSSA, 2014

Evidence for Subsidiary Faults

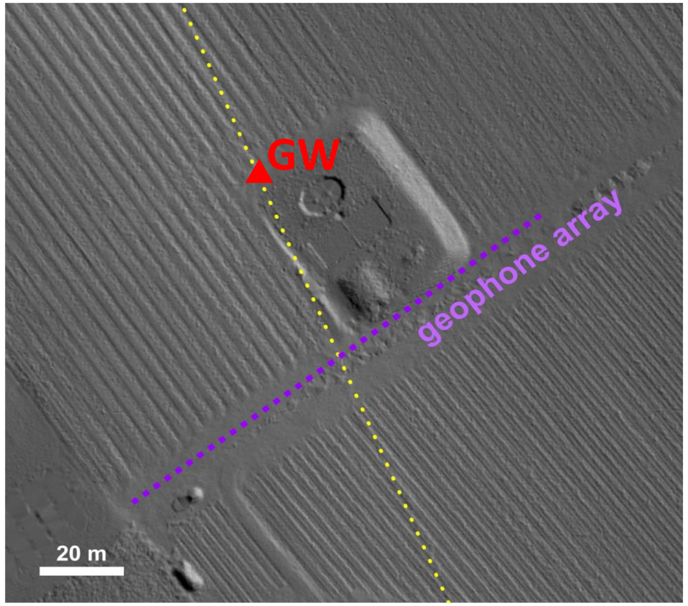

Why did fault slip focus onto one strand?

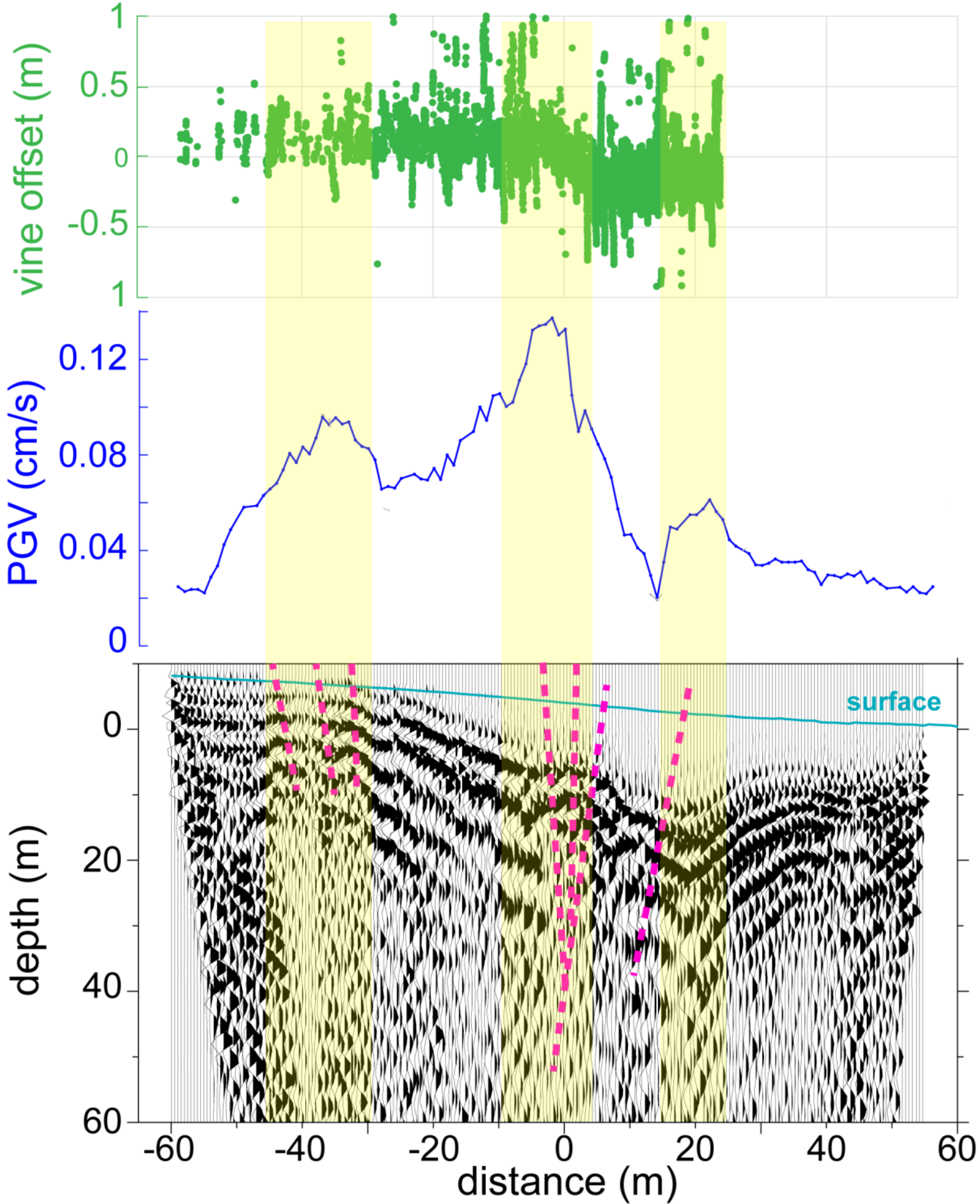

Evidence for compliant zone from refraction tomography

- High fracture density → Reduced s-wave velocity
- Fluid saturation → Increased p-wave velocity

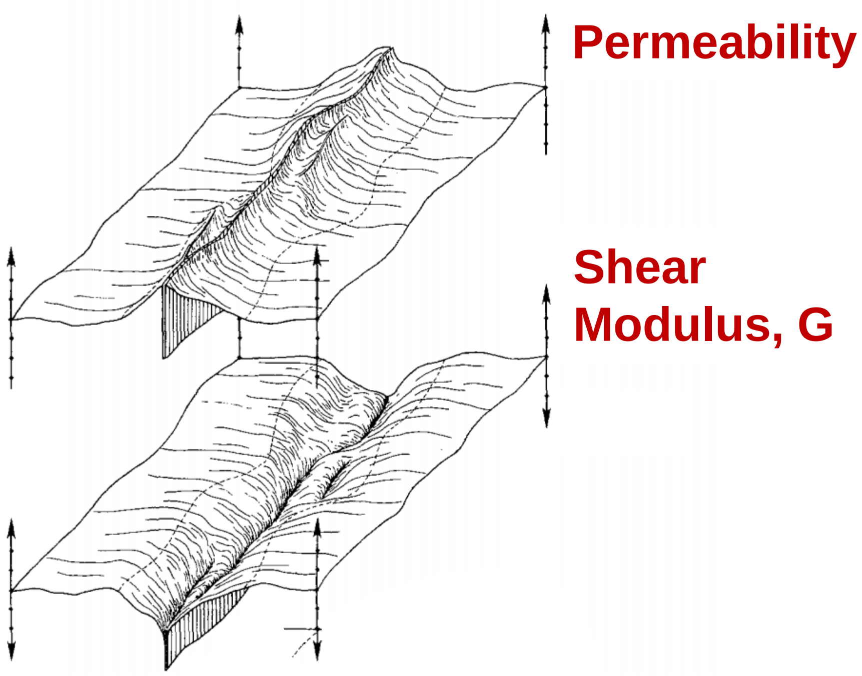

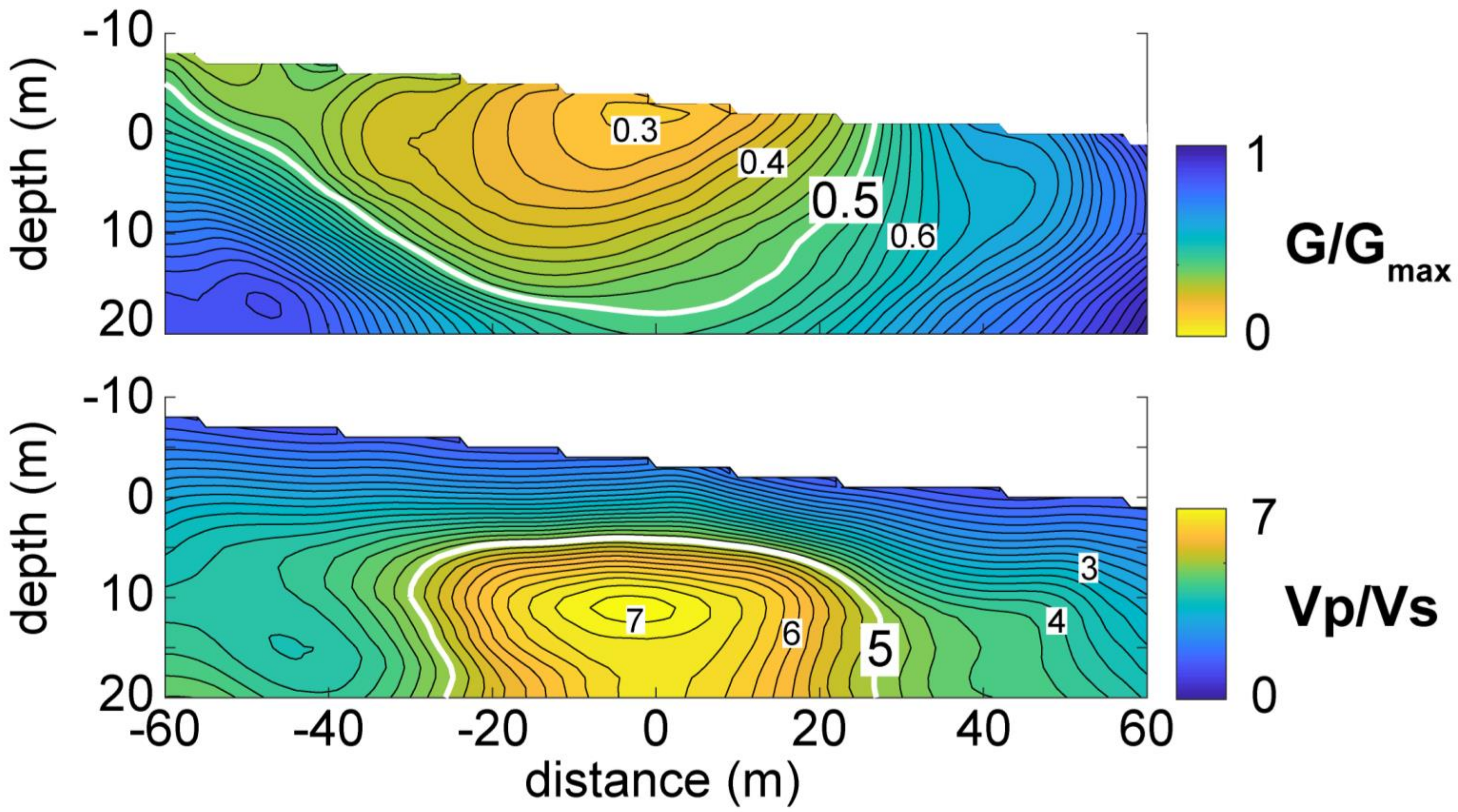

Chester & Logan [1986]

Variation in subsurface structure and mechanical properties

Post-seismic Site **Co-seismic Site**

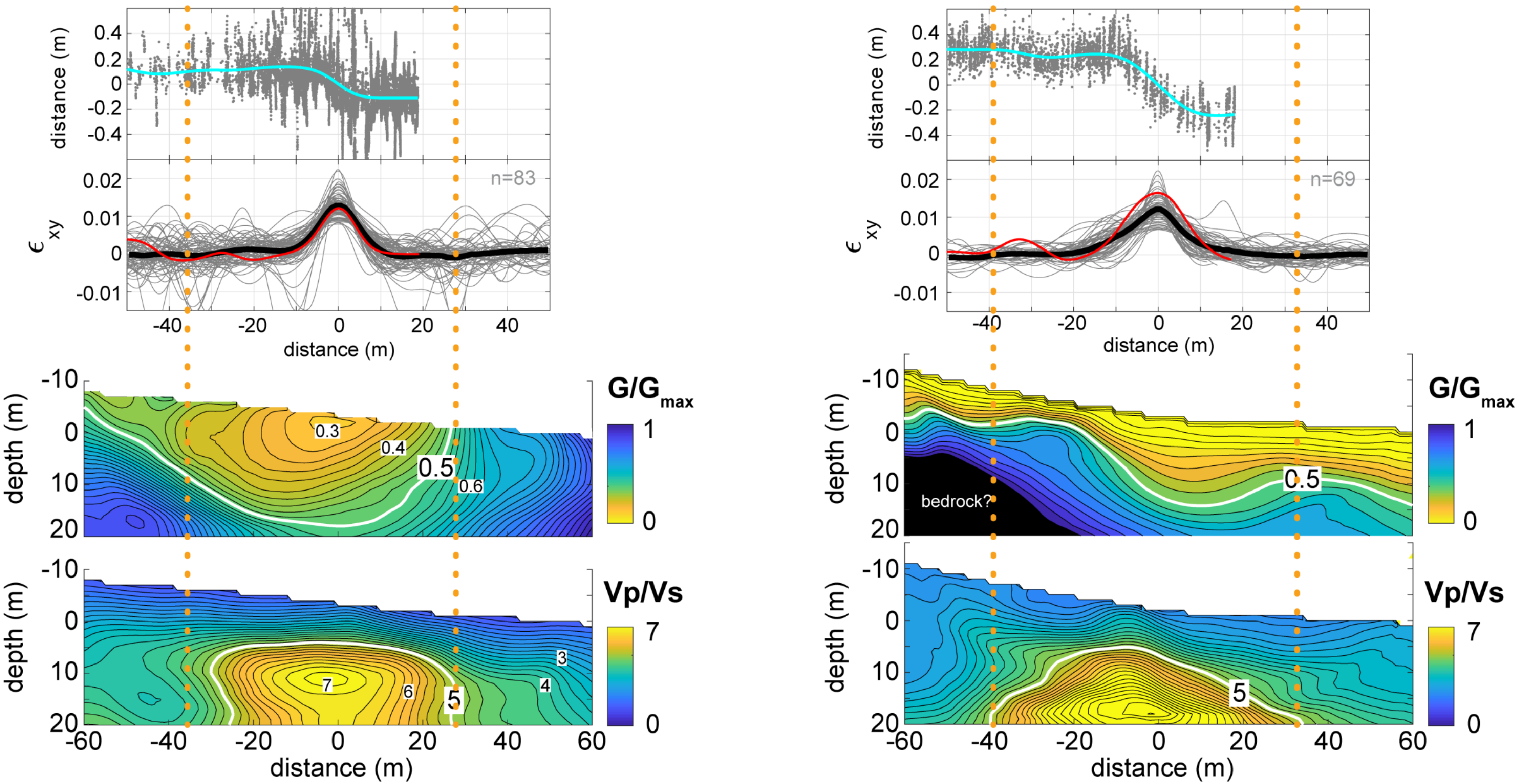

Formal inversion for shallow fault slip using MLS data

PARAMETERS

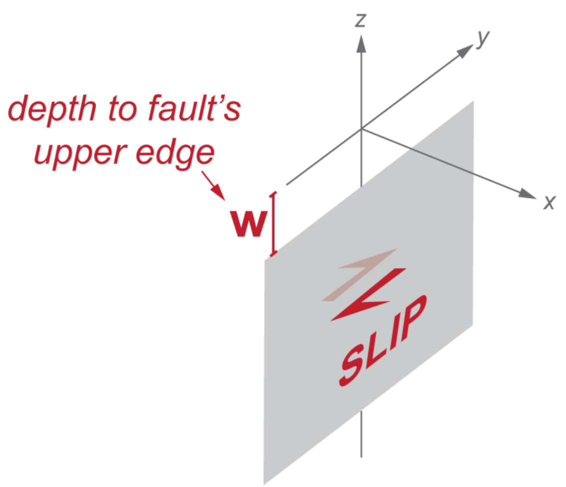

Gm = d

DATA

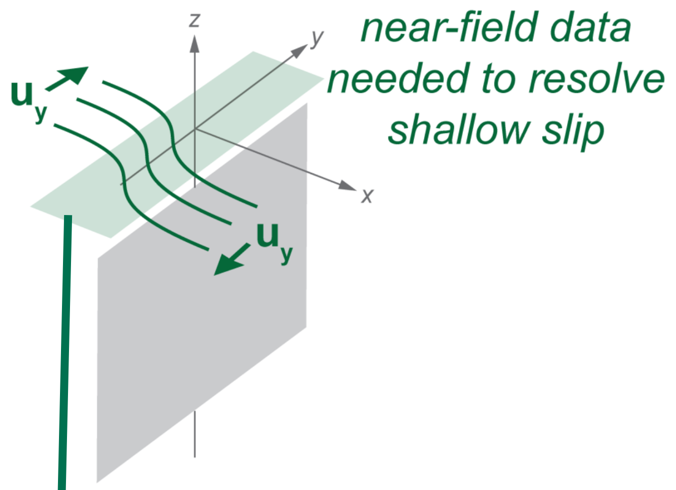

ELASTIC MODEL

slip

depth to upper edge

$$u_y = (s/\pi)*[\tan^{-1}(y/W)-\tan^{-1}(y/w)]$$

surface displacement

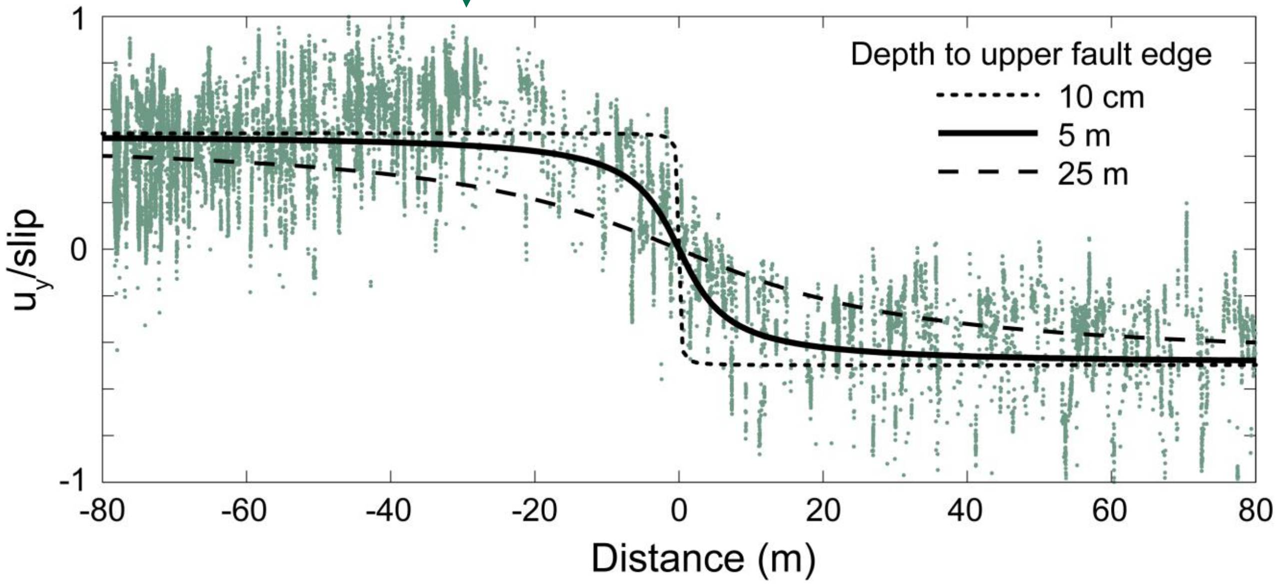

Inferred slip (0.5-1.25 m) at shallow depths (3-25 m)

Post-seismic Site

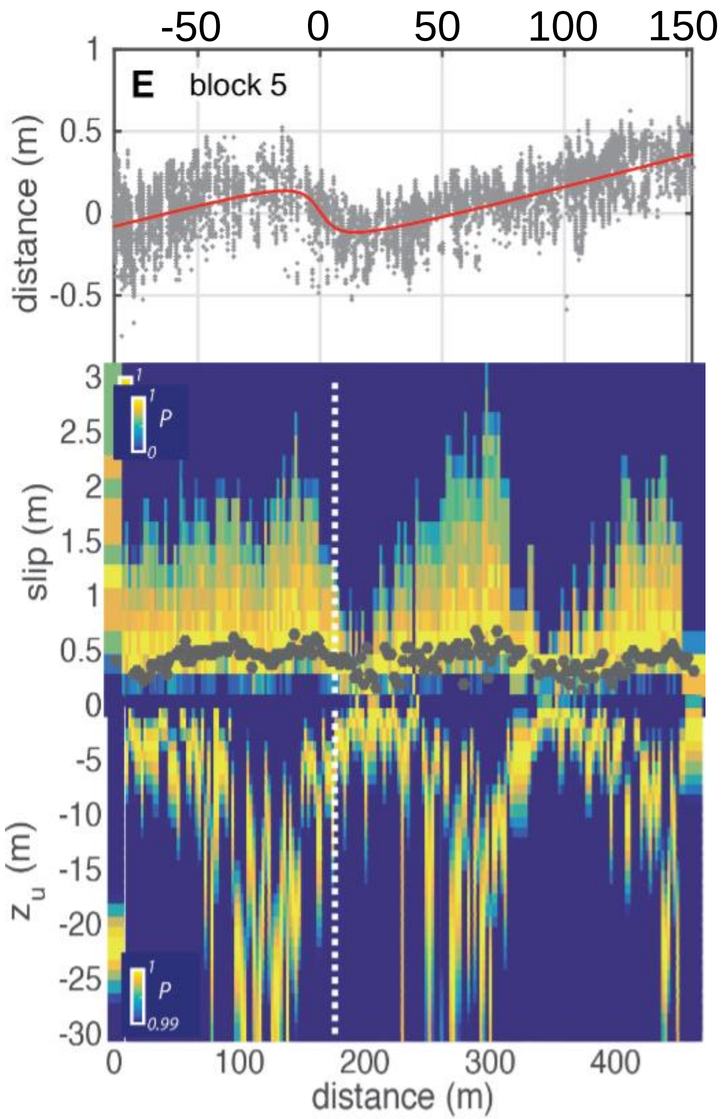

Co-seismic Site

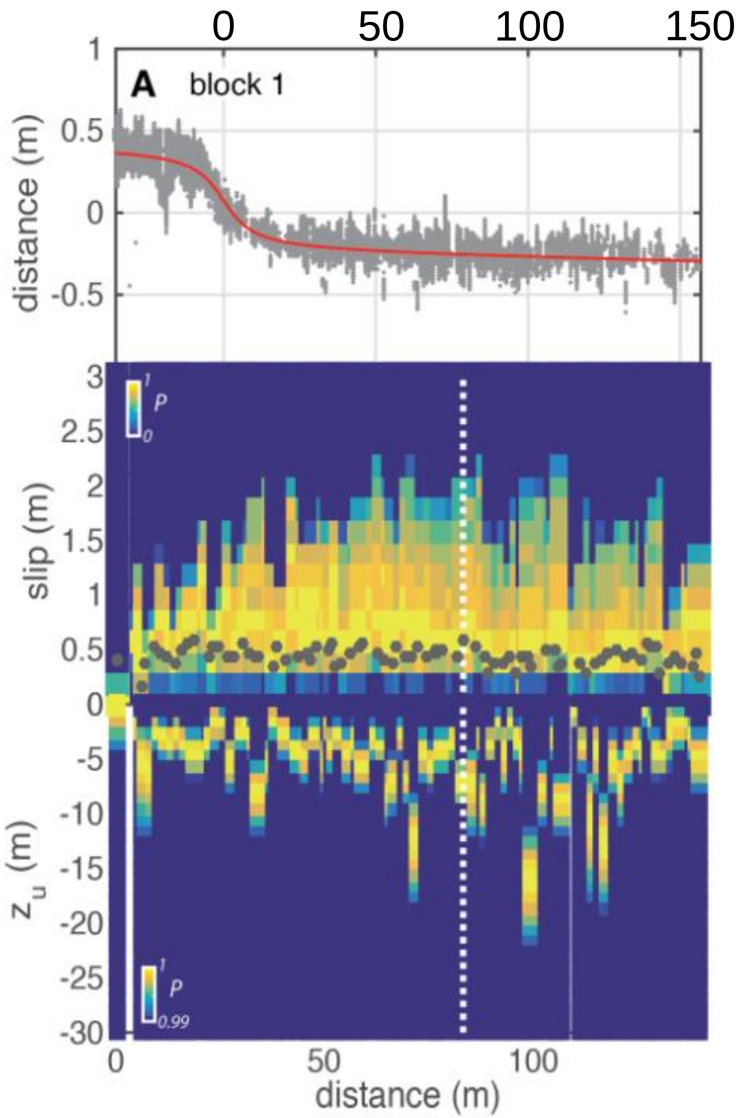

Along-strike summary

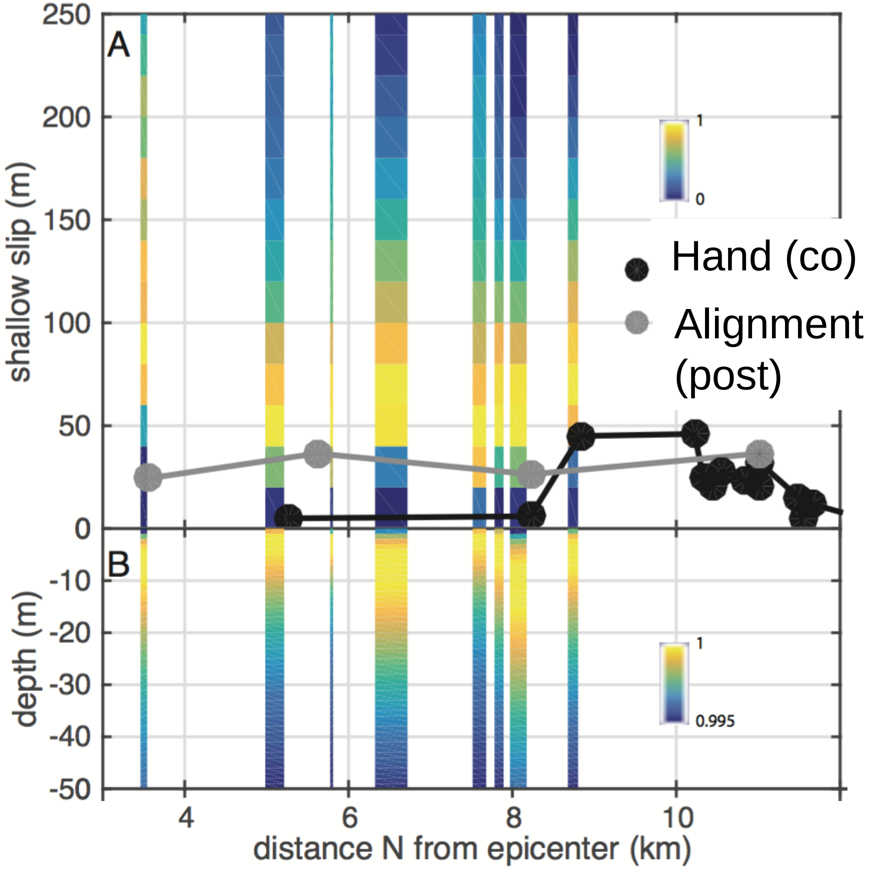

Brooks et al. [accepted, *Science Advances*]

Abaqus Finite Element Software

- **Commercial multi-physics modeling package**
  - Abaqus/Standard – Implicit, quasi-static deformation
  - Abaqus/Explicit – Explicit, dynamic deformation
  - Abaqus/CFD – Computational fluid dynamics
  - Abaqus/CAE – GUI to build models, submit analyses, monitor jobs, evaluate results
  - Abaqus/Viewer – Post-processing and visualization

- **Many built-in constitutive behaviors**
  - *Elastic*: Isotropic/Anisotropic, Hyperelastic, Poroelastic…
  - *Elastoplastic*: Von Mises, Mohr-Coulomb, Drucker-Prager, Cam-Clay, Damage …
  - *Creep and Viscoelastic*: Linear, Power-law, Exponential…
  - *Elastoviscoplastic*: Coupled, Two-layer…

- **Targeted toward engineers**
  - Increasingly used in earth sciences, but documentation still lacking.

Complete Abaqus Environment (CAE)

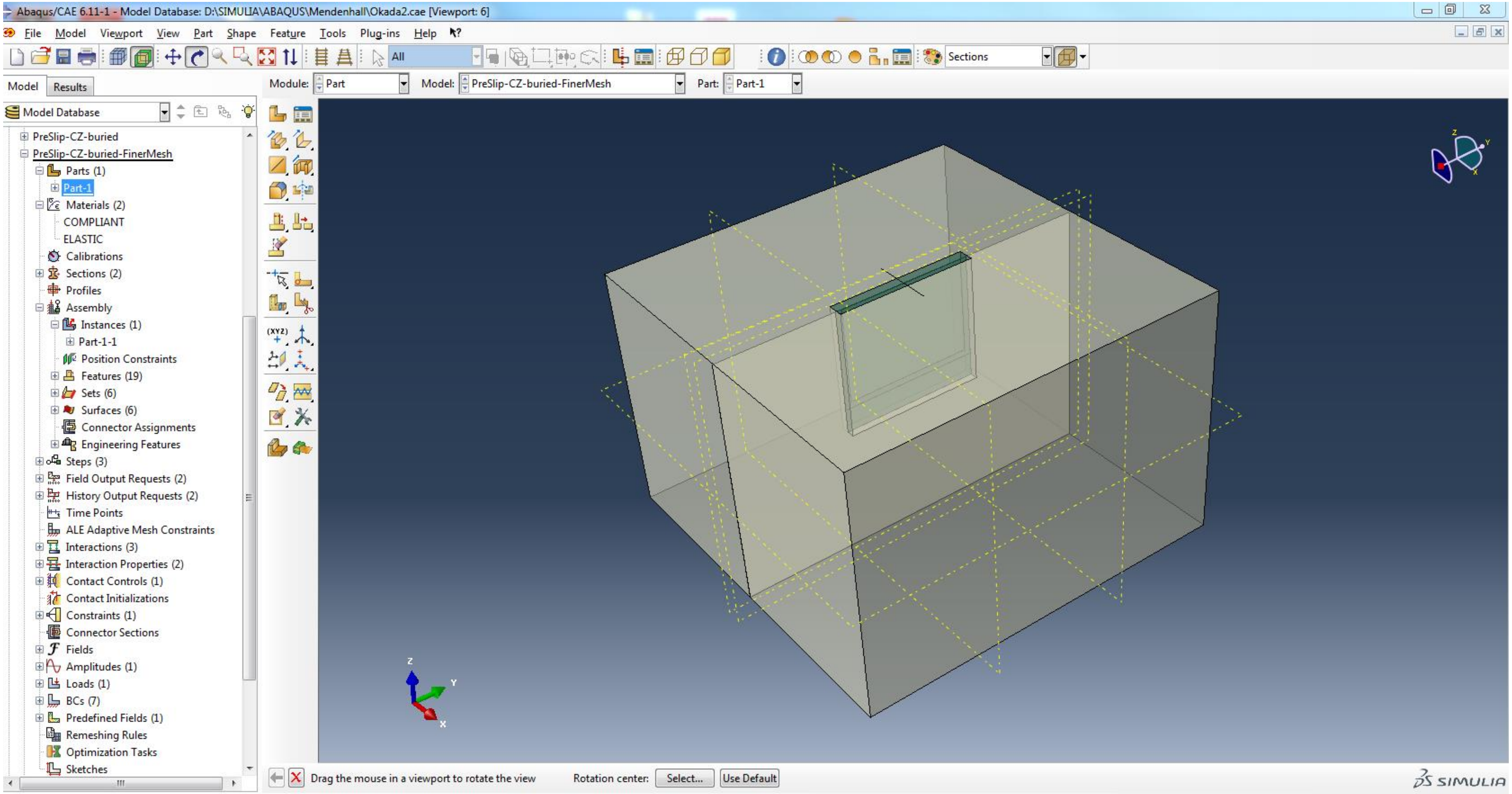

Modeling faults in Abaqus

- **"Crack Seam" tool**

  Works well for remote loads or applied tractions

  Cannot prescribe displacement

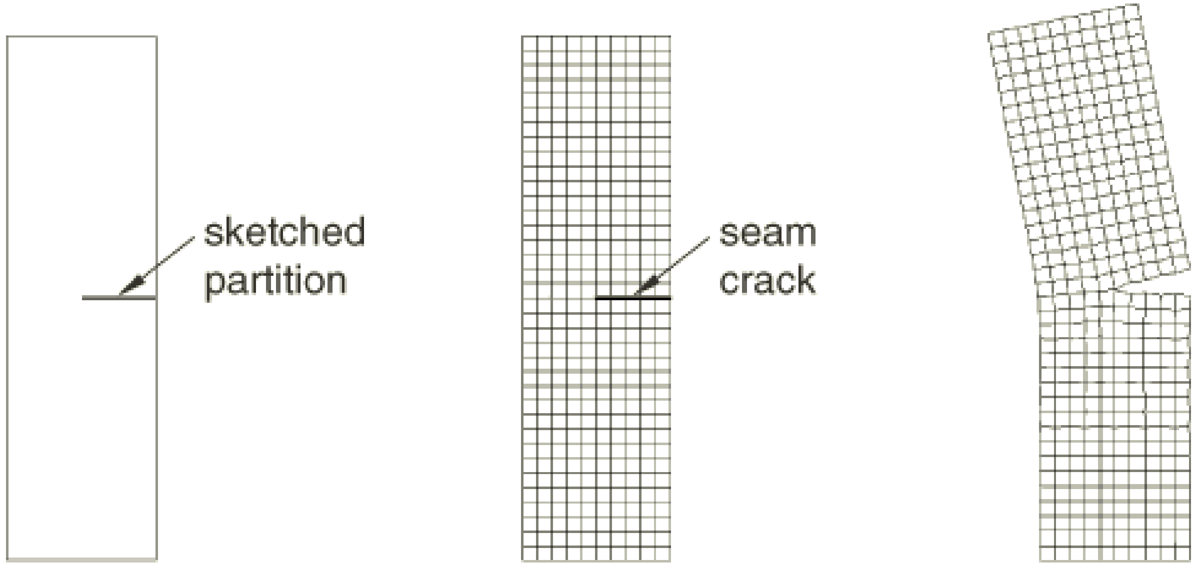

- **High aspect-ratio triangular cuts**

  Can be used with either displacement or traction BCs

  Meshing can be very difficult, computationally expensive

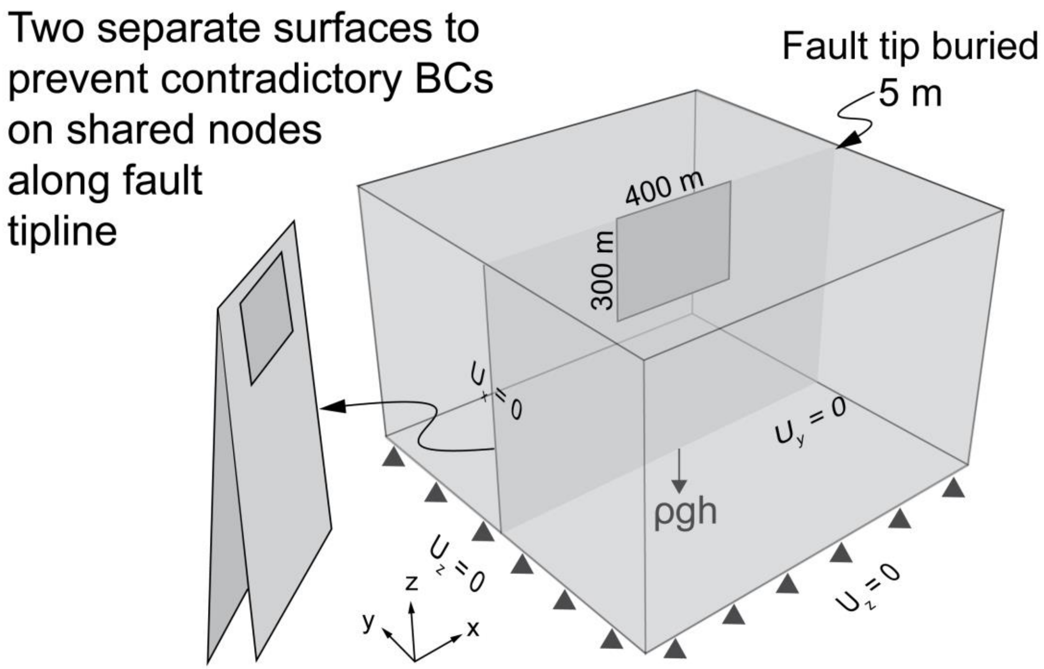

2. How sensitive is shallow deformation to constitutive properties?

Homogeneous Elastic
(e.g., Okada, 1985)

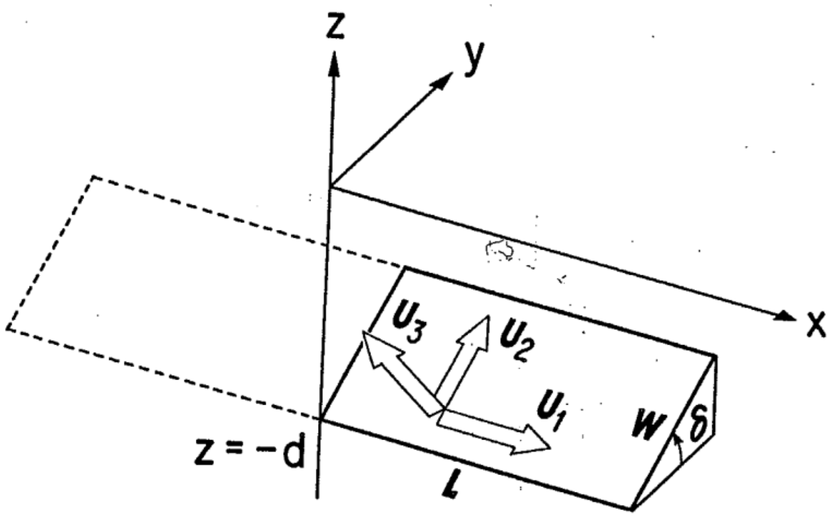

Compliant Zone Elastic
(e.g., Barbot et al., 2008)

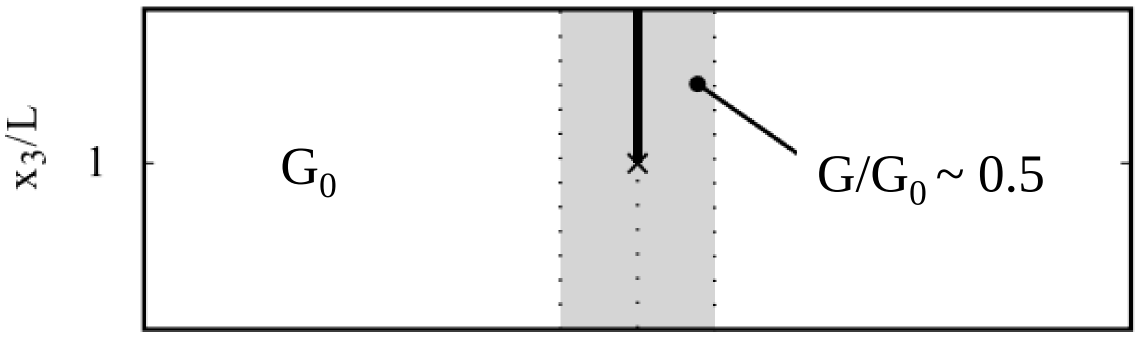

Elastoplastic
(e.g., Kaneko & Fialko, 2011)

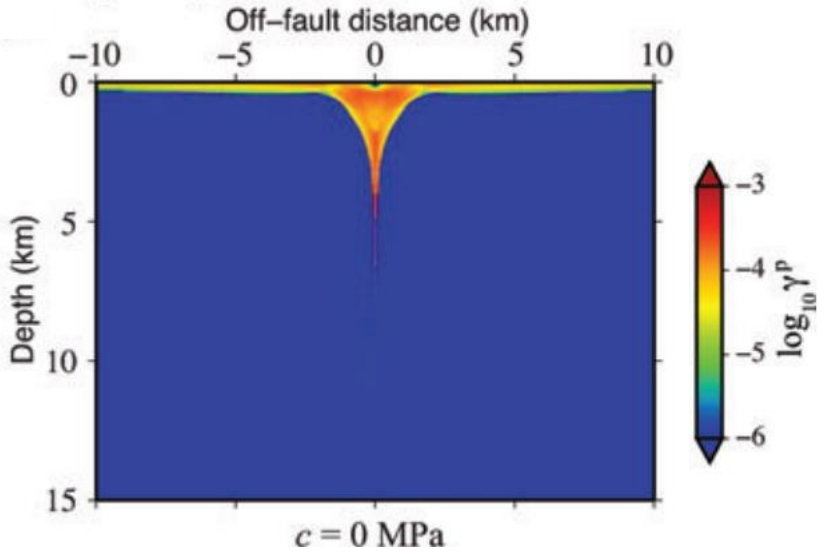

Drucker-Prager Elastoplasticity

Cohesion (*C*): Non-frictional part of shear-resistance.

Low *C* = Gravel (0 kPa)
High *C* = Clay (100 kPa)

Angle of Internal Friction (*φ*): Imparts dependence on normal stress

Low *φ* = Compacted clay (15°)
High *φ* = Densely packed, angular sand/gravel (45°)

Base Case estimates for Napa:
C = 50 kPa, φ = 25°, μ_{fault} = 0.4
E = 100 MPa, ν = 0.3, ρ = 2000 kg/m^3

Yield Envelope

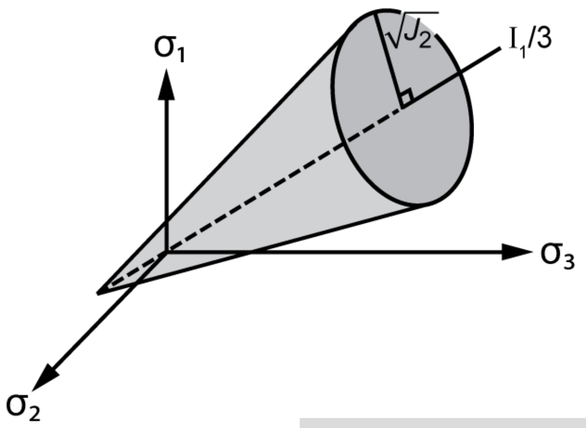

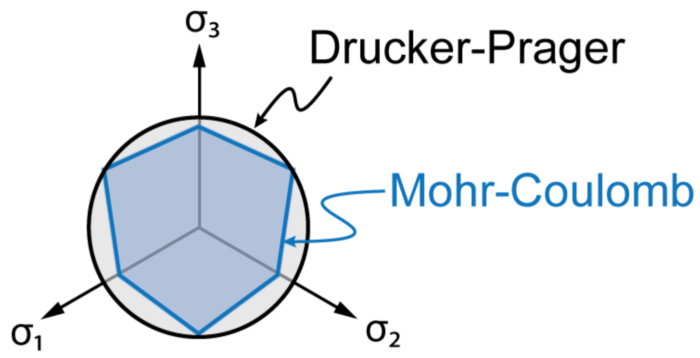

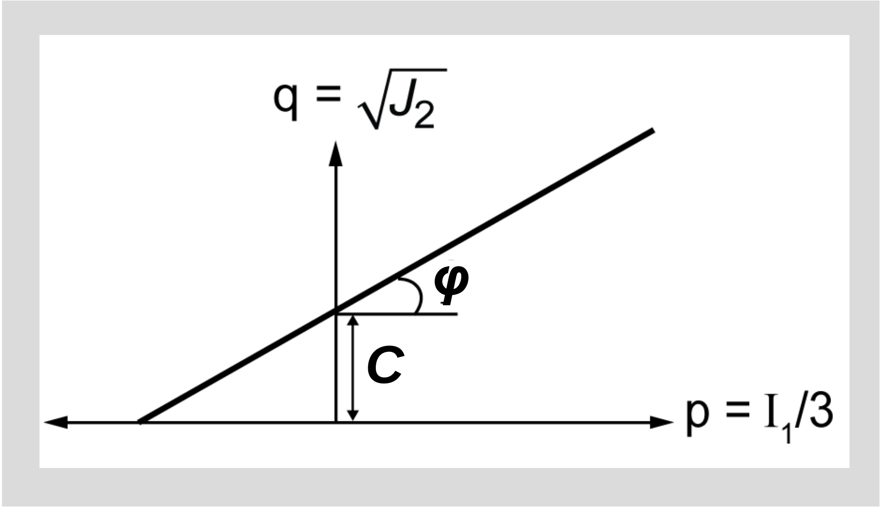

C –***COHESION***
φ –***ANGLE OF INTERNAL FRICTION***

Model geometry, mesh, and boundary conditions

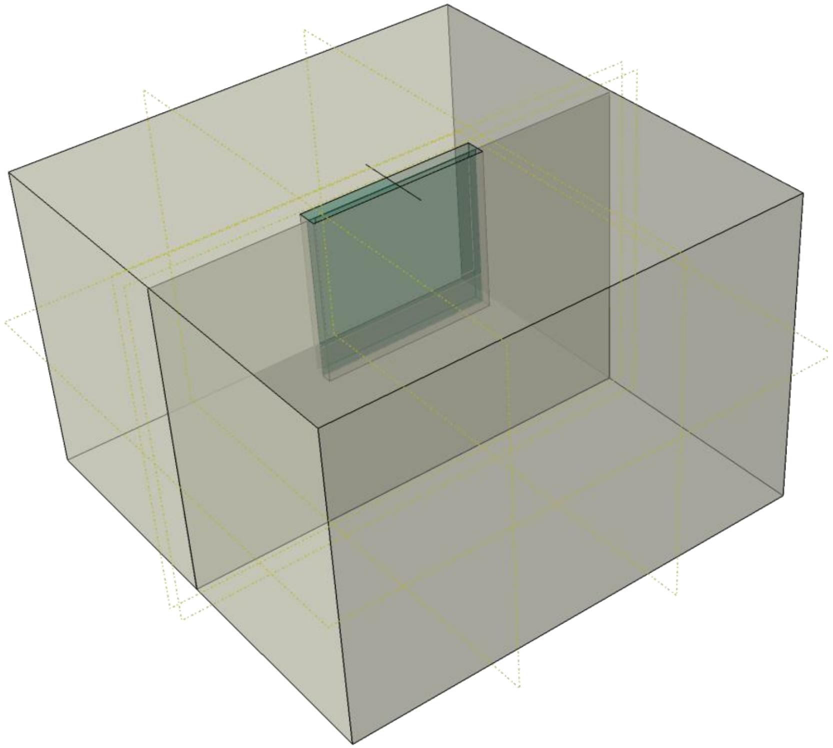

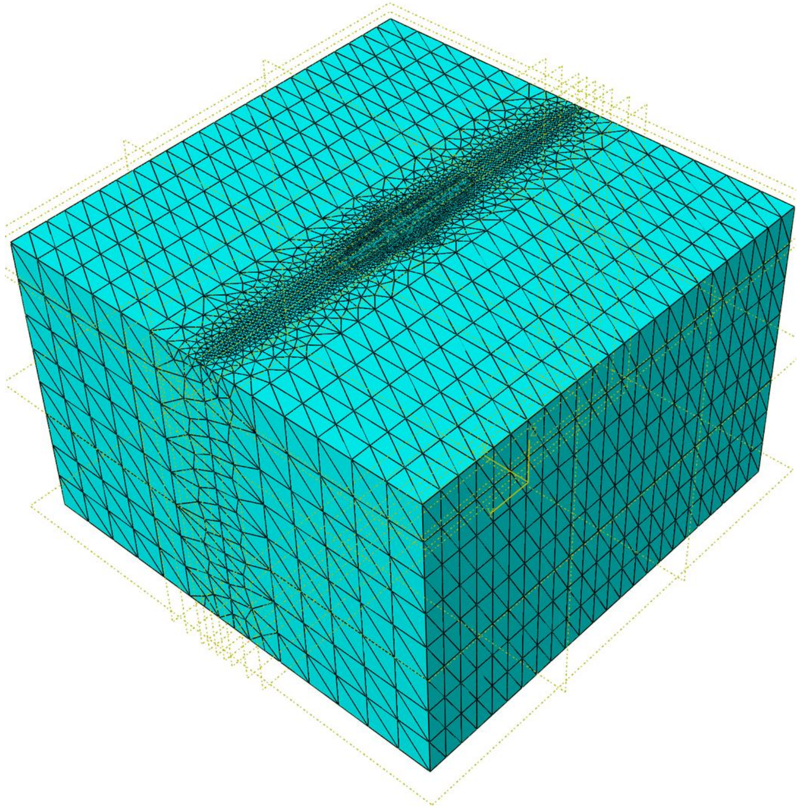

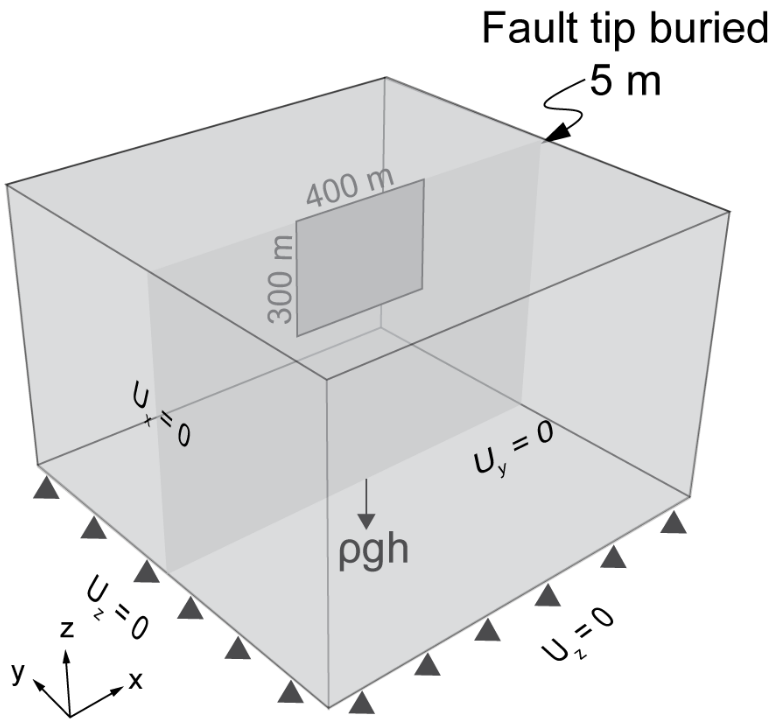

<u>Model domain:</u>
1000 m x 1000 m x 800 m

<u>Fault dimensions:</u>
300 m x 400 m, buried 5 m

<u>Compliant zone:</u> +/- 25 m

<u>Mesh:</u>
160,000 linear tetrahedrals
Size range: 0.5-50 m

<u>Loading</u>
Initial: Geostatic stress

Step 1: Gravitational load

Step 2: Uniform slip = 1 m
(Prescribed slip)

Effect of constitutive properties

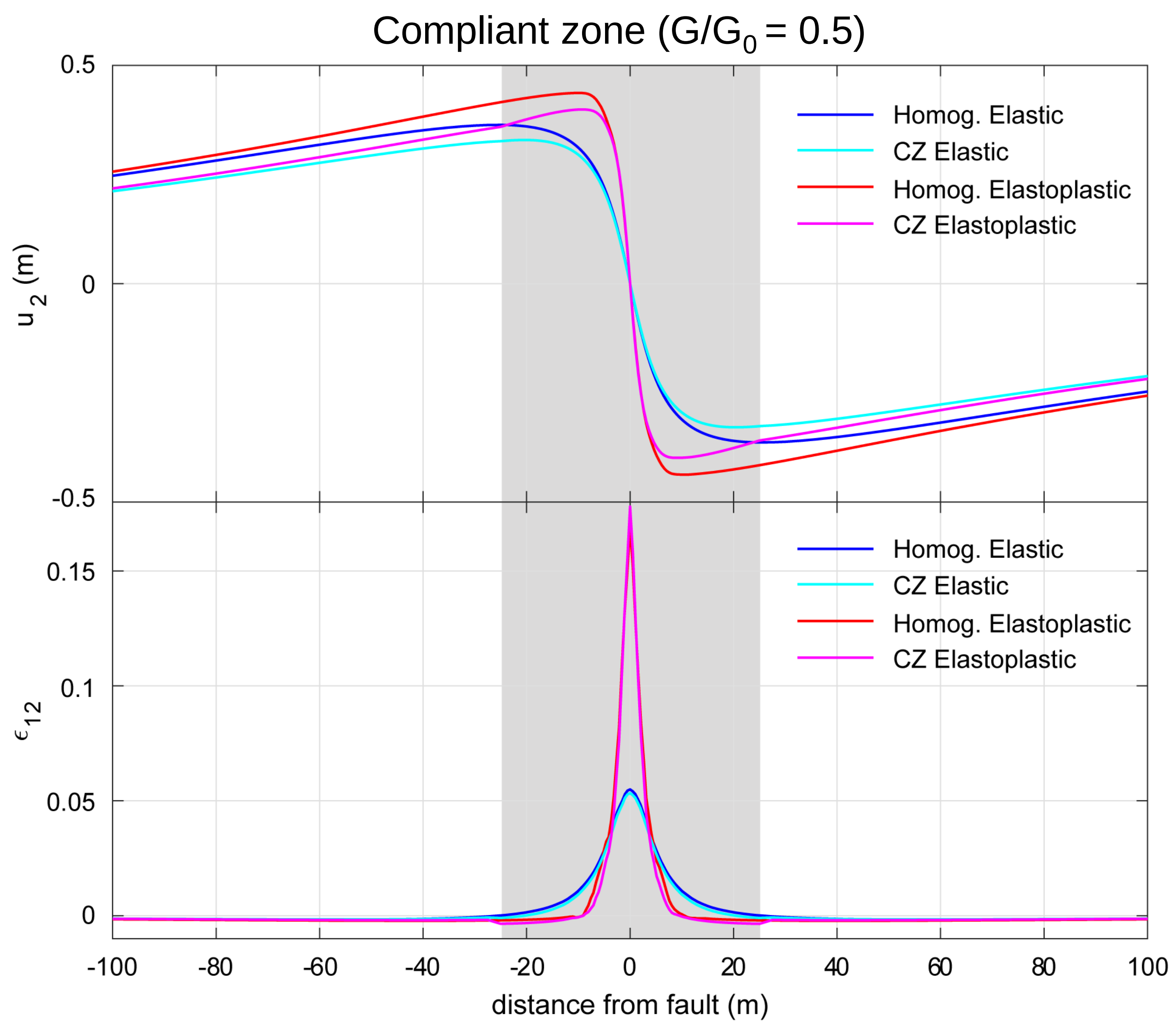

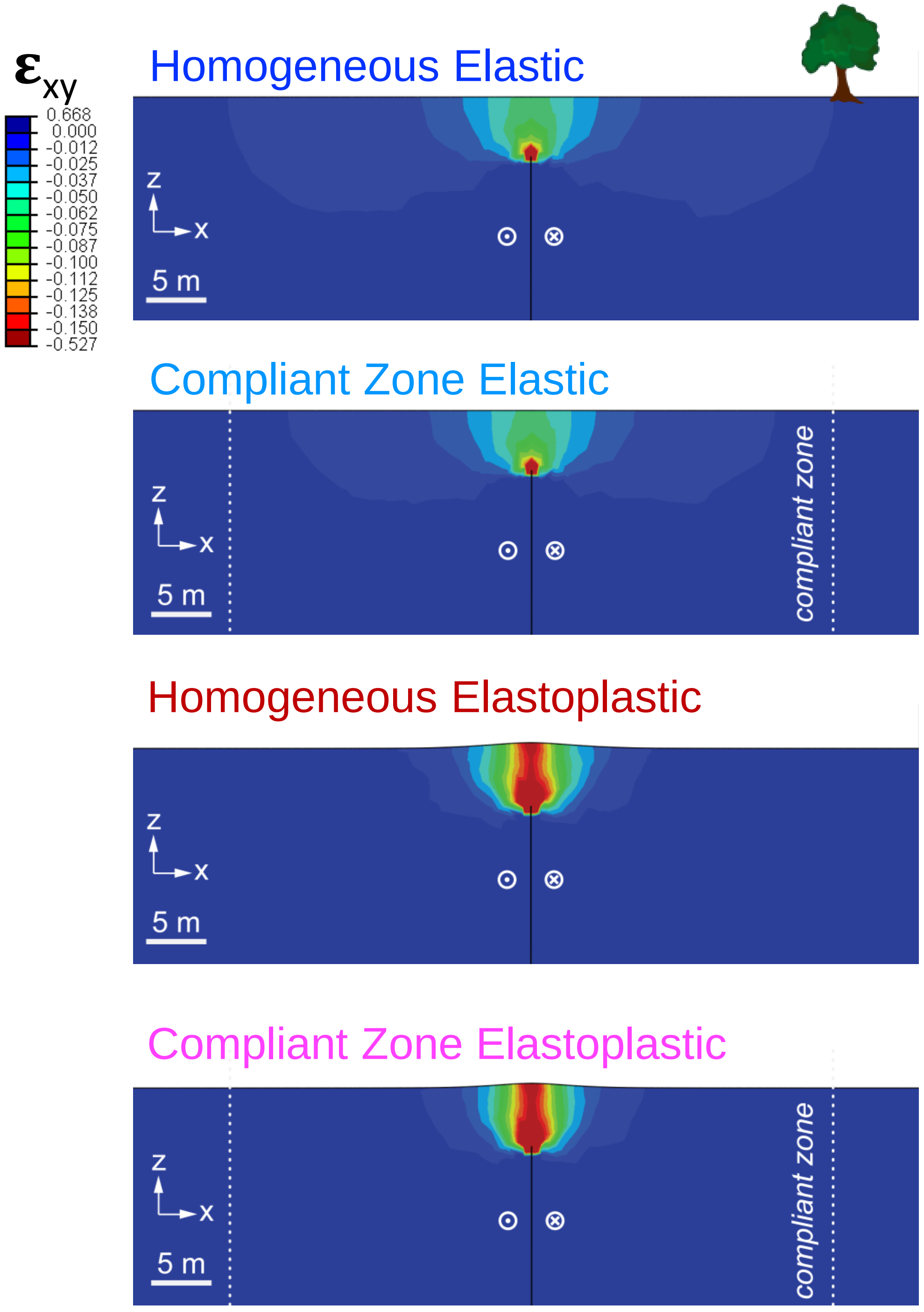

Comparison of model results with MLS data

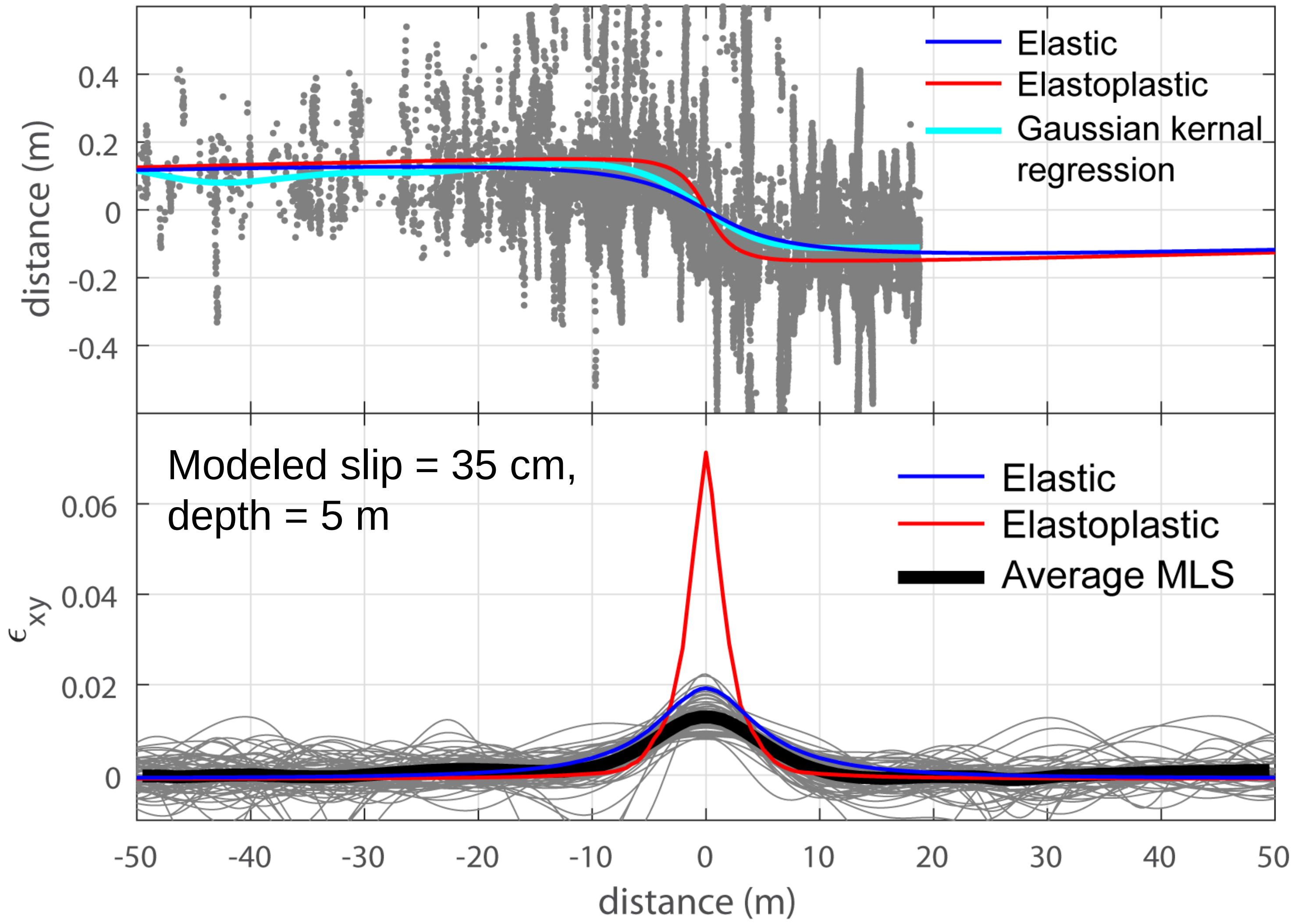

Non-uniqueness

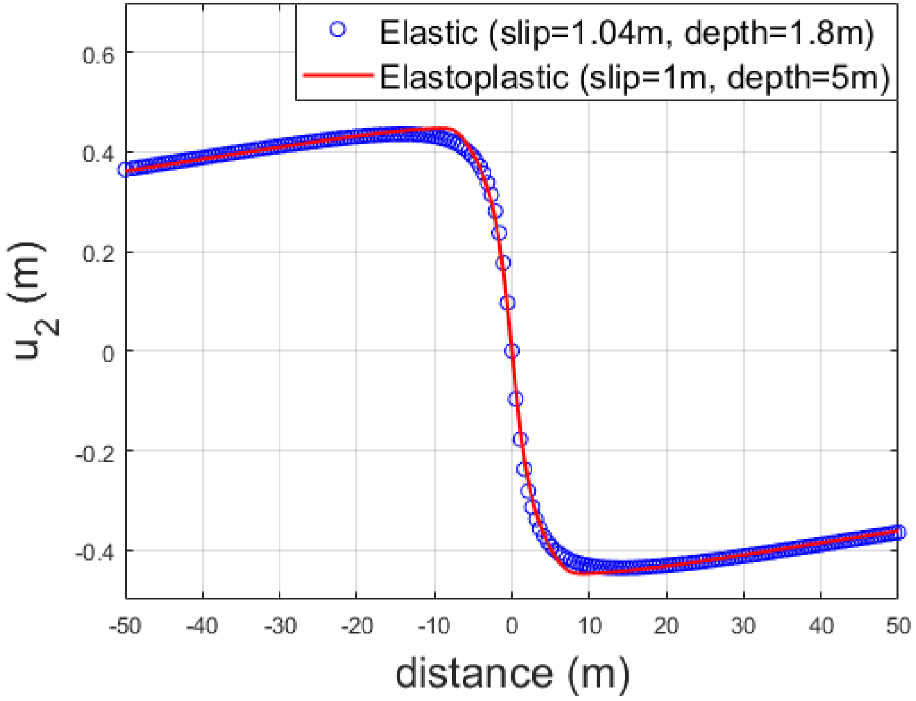

Ave. Residual = 0.6 cm

Not detectable by MLS

Elastoplastic model with remote loading (spontaneous rupture)

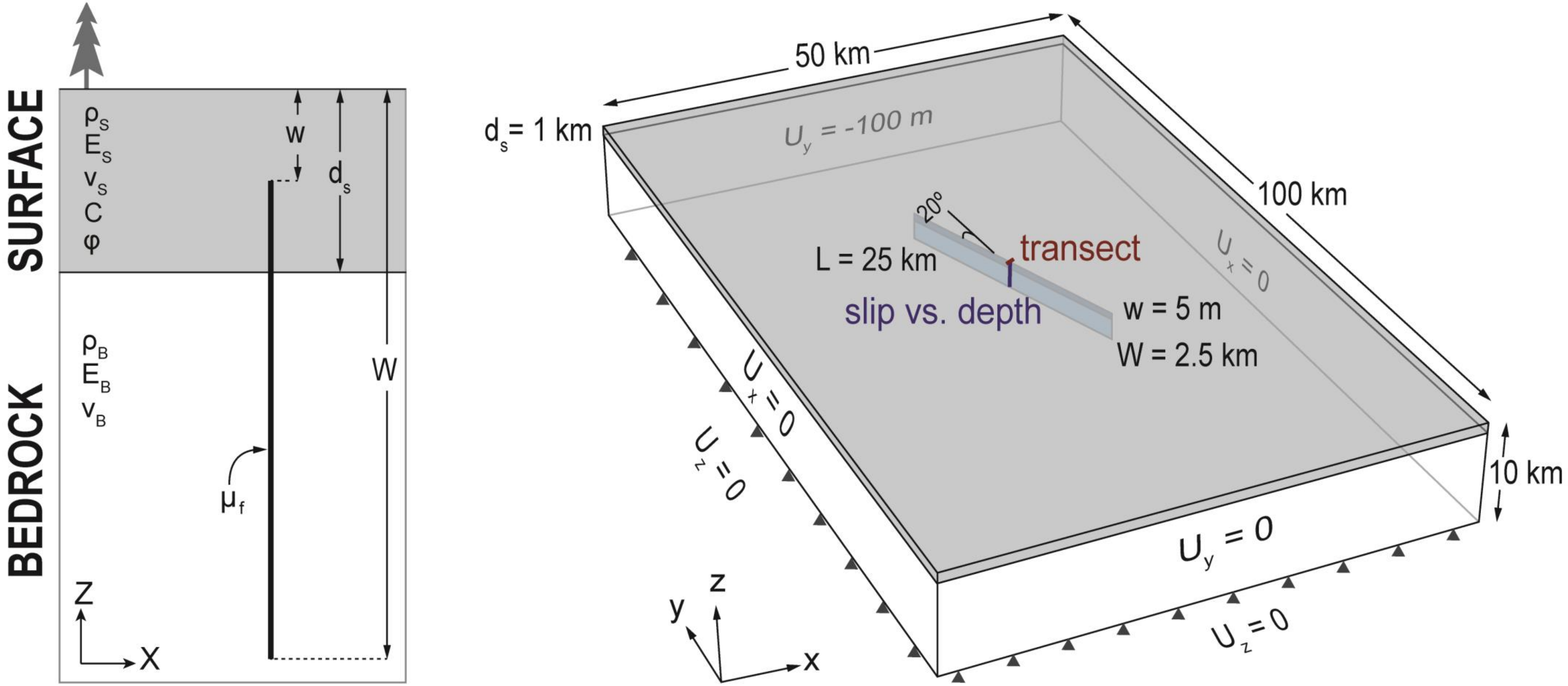

- Elastoplastic surface layer overlying elastic basement
- Remote displacement boundary conditions (transpression) with gravity
- Fault slip governed by Coulomb criterion: $\boldsymbol{\sigma_s = \mu\sigma_n}$

Effect of cohesion on fault slip and surface deformation

Plastic shear strain:

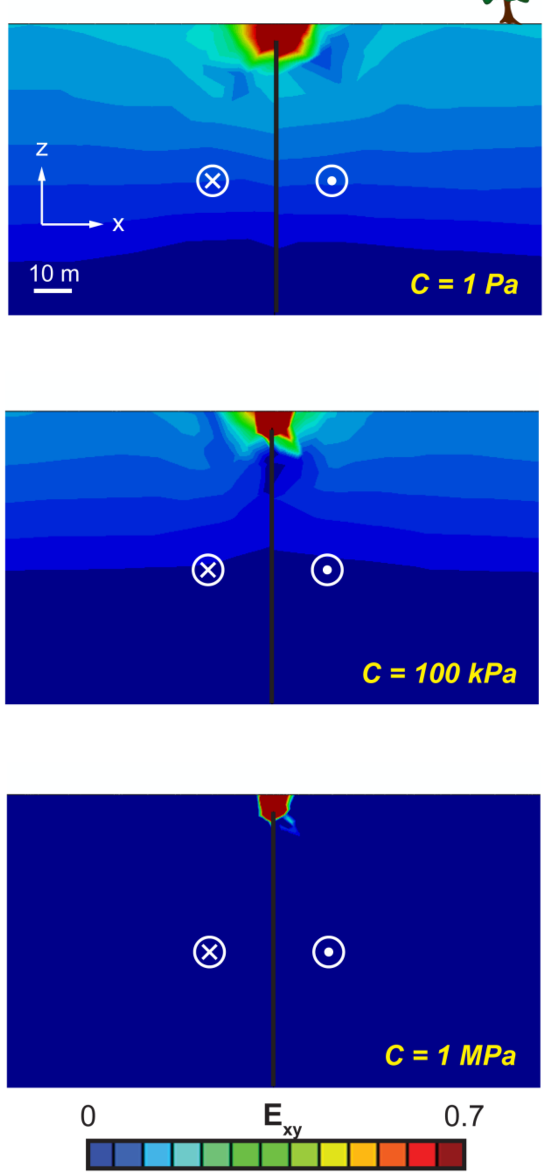

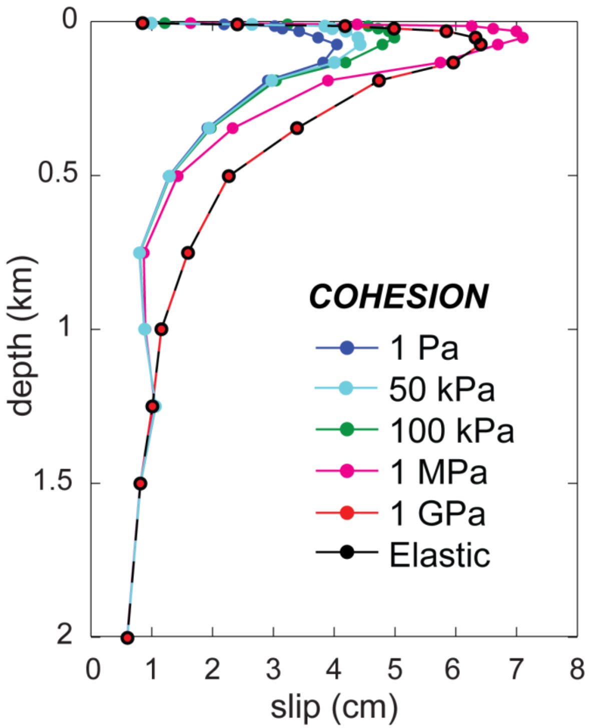

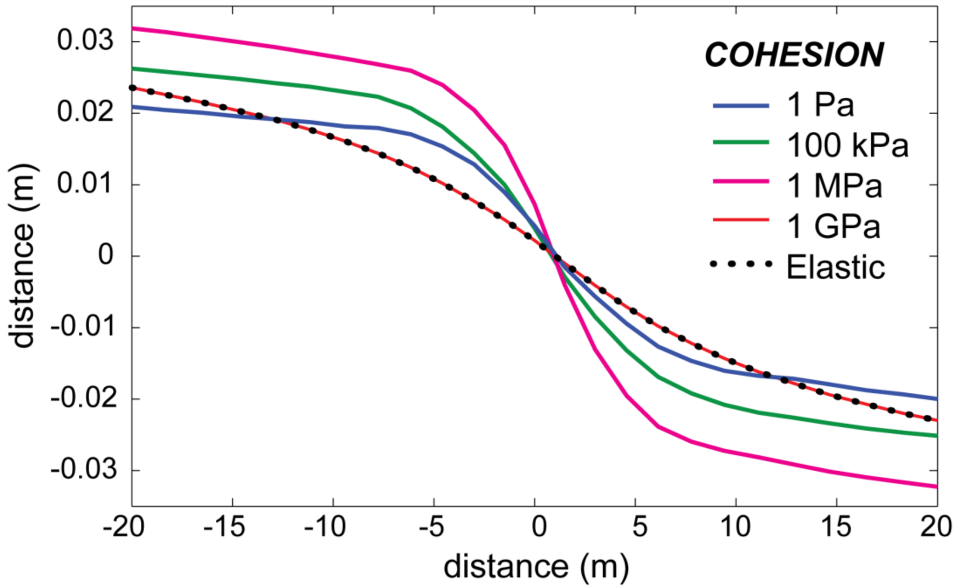

- Lower cohesion produces greater regions of off-fault plasticity, relaxing stress on the fault

- Slip and shear localization at the surface increase with increasing cohesion

Effect of Cohesion: Comparison to field examples

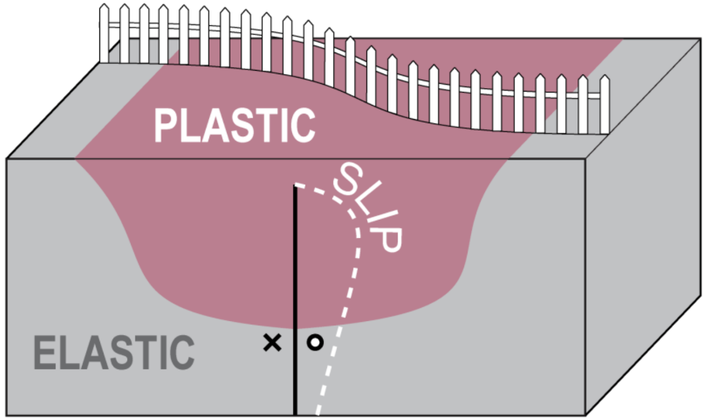

LOW COHESION (e.g., gravel)

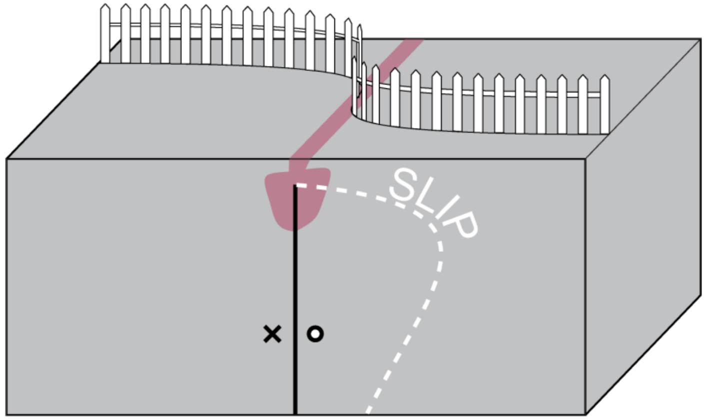

INTERMEDIATE COHESION (e.g., soil)

thick gravel deposit

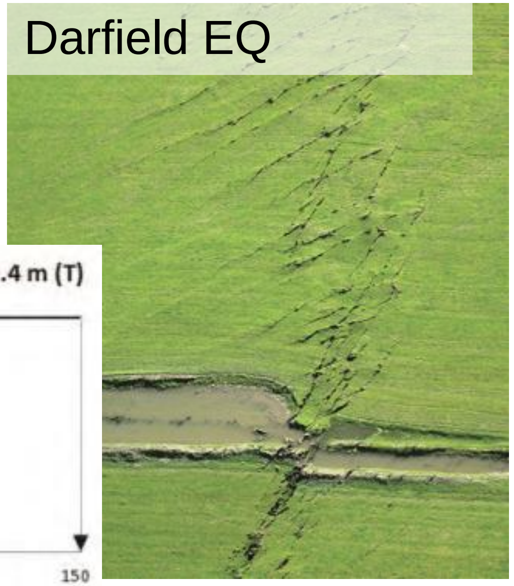

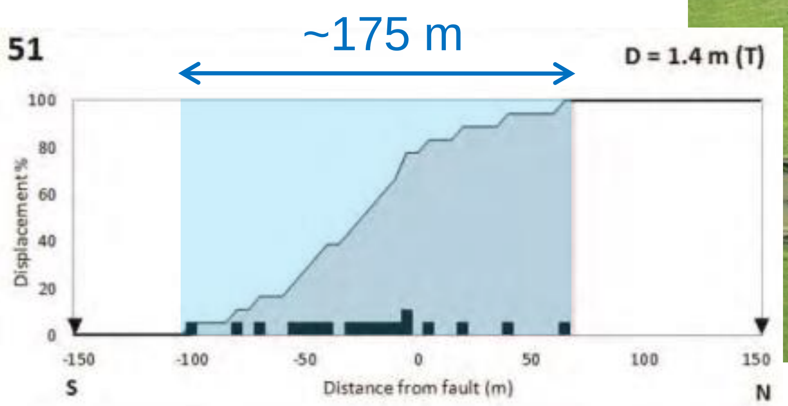

Litchfield et al. [2014]

Quigley et al. [2012]

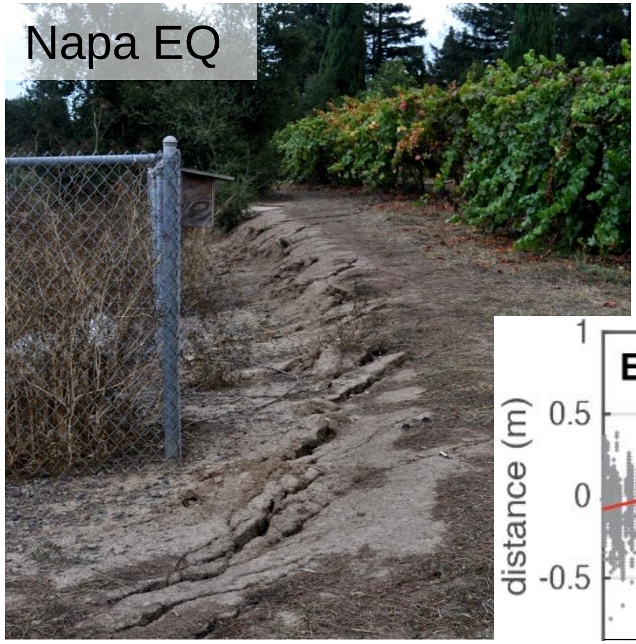

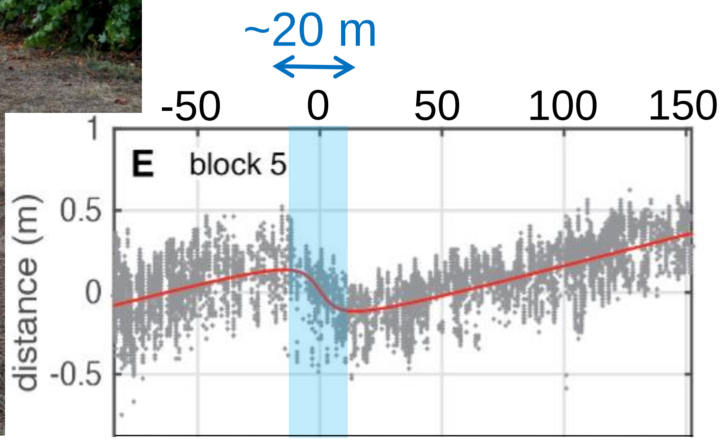

Conclusions

- What is the magnitude and distribution of shallow fault slip?
  - Along S. Napa rupture, significant slip (0.5-1.25 m) at shallow depths (3-25 m)
  - Greater than surface measurements, but still less than than finite fault models suggest.

- How sensitive is shallow deformation to constitutive properties?
  - For the model same inputs (slip and burial depth), surface displacements are much more sensitive to variation in plastic parameters than to compliant zone parameters.
  - Surface displacement measurements and subsurface seismic imaging show that deformation is focused to a much narrower region than the compliant zone width.

- Can surface deformation reveal rupture dynamics?
  - For Napa, predominantly co- and post-seismic sites show very similar deformation patterns.
  - Rupture may have slowed down such that dynamic stress ≈ static stress field.

- Questions raised:
  - Why would a rupture arrest within meters of Earth’s surface?
  - Why are some fault strands activated over others?
  - What mechanisms contribute to distributed shear deformation?

Upcoming activities

- Collect core samples for microstructural analysis and mechanical testing

Post-seismic Site

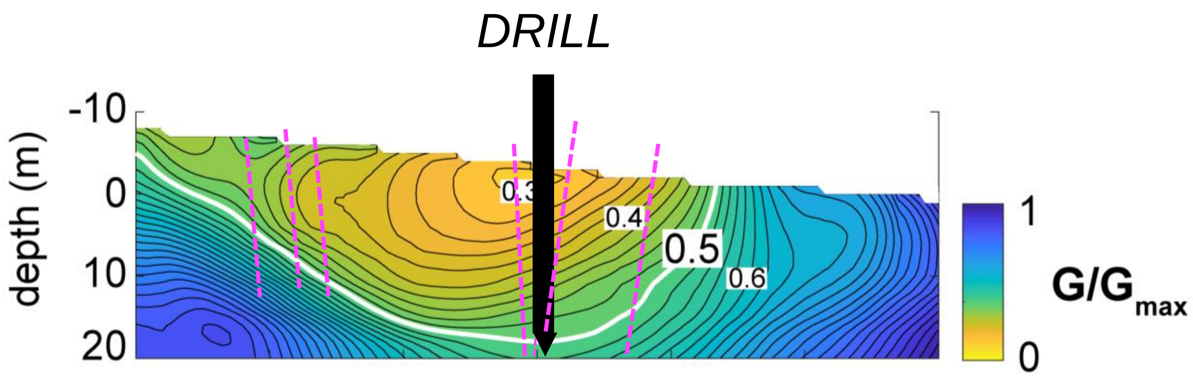

Coseismic Site

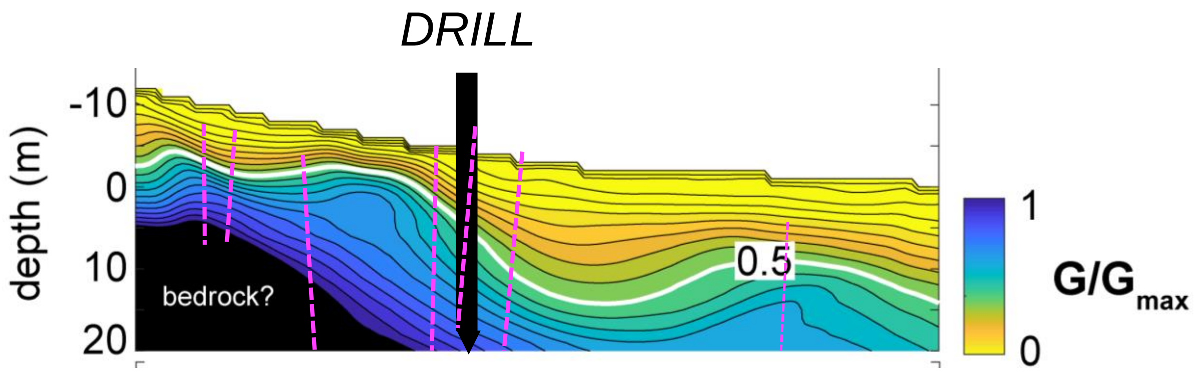

AGU FALL MEETING

New Orleans | 11–15 December 2017

G013:
Near-Surface Structure and the Mechanics of Shallow Fault Slip

Co-Organized with:
Geodesy, Seismology, and Tectonophysics

WED 2 AUG : Abstract Submissions Deadline